

Summer 2016

Low-Cost Quartz Crystal Microbalance System Platform Designed for Chemical Nanoparticle

Danming Wei

Western Kentucky University, danming.wei011@topper.wku.edu

Follow this and additional works at: <http://digitalcommons.wku.edu/theses>



Part of the [Analytical Chemistry Commons](#)

Recommended Citation

Wei, Danming, "Low-Cost Quartz Crystal Microbalance System Platform Designed for Chemical Nanoparticle" (2016). *Masters Theses & Specialist Projects*. Paper 1635.
<http://digitalcommons.wku.edu/theses/1635>

This Thesis is brought to you for free and open access by TopSCHOLAR®. It has been accepted for inclusion in Masters Theses & Specialist Projects by an authorized administrator of TopSCHOLAR®. For more information, please contact topscholar@wku.edu.

LOW-COST QUARTZ CRYSTAL MICROBALANCE SYSTEM PLATFORM
DESIGNED FOR CHEMICAL NANOPARTICLE ANALYSIS BASED ON ARDUINO
MICROCONTROLLER BOARD

A Thesis
Presented to
The Faculty of the Department of Chemistry
Western Kentucky University
Bowling Green, Kentucky

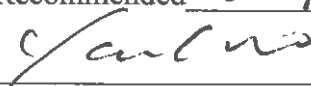
In Partial Fulfillment
Of the Requirements for the Degree
Master of Science

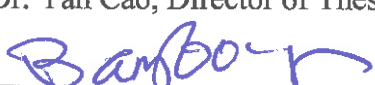
By
Danming Wei

August 2016

LOW-COST QUARTZ CRYSTAL MICORBALANCE SYSTEM PLATFORM
DESIGNED FOR CHEMICAL NANOPARTICLE ANALYSIS BASED ON ARDUINO
MICROCONTROLLER BOARD

Date Recommended July 25, 2016


Dr. Yan Cao, Director of Thesis


Dr. Bangbo Yan


Dr. Darwin Dahl


Dean, Graduate School

7/29/16
Date

I dedicate this thesis to my parents, Chang Wei and Lizhi Guo, who are a great inspiration to me. Also, I also dedicate this work to my advisor Yan Cao, who helped greatly in research process and editing this manuscript.

ACKNOWLEDGMENTS

I am taking this opportunity to express my special appreciation to my thesis advisor Dr. Yan Cao. He has been a great mentor for me. I am really thankful for his patient guidance, and serious but invaluable criticism during these two years. I would like to thank for his aspiring and encouraging my research work and leading me to grow to be a scientist. He gave me invaluable constructive suggestions and friendly advices on both of my research work, my career, and life, leaving me a priceless benefits and influences in my future life. I would also like to thank him for sharing his brilliant and illuminating ideas and views on a numerous questions and issues related to the research works.

I am also sincerely grateful to my committee members, Dr. Yan Cao, Dr. Bangbo Yan, and Dr. Darwin Dahl. I would like to thank them for those helpful comments and suggestions on the thesis revision, and giving me an enjoyable defense time.

I would express my gratitude to my work partners who provide me a lot technique help and constructive suggestions. This appreciation will send to Ying Chen, Jiao Wang, Jinyi Yue, Kolton Jones and many others.

Finally, a special appreciation is for my family supporting me all the time without any rewards.

PREFACE

I have strong curiosity to explore the unknown's parts in the world. The mysterious and colorful world gives me a great motivation and power, I made a decision to be a scientist, and I would keep learning and searching knowledge and answers of this world.

Chemistry is a fantastic area, which can present mechanism and features of the world. I am obsessed by chemistry and choose it as my major. Also I believe there exist connections across different academic fields, like physical chemistry, biochemistry, and electrochemistry and so on. The research work gives me a great opportunity to get close to explore the relationship between electronic instrument and chemical analysis. Through designing an electronic platform based on QCM sensor properties, to explore and understand micro-world. I tried my every effort to figure out the questions and problems that I met. This was a big challenge for me to research a new academic field, but I am still excited to learn what I have never learnt before.

I have a great deal of enthusiasm about the research work, and I enjoy the learning and studying process. I really hope my work would be valuable and useful in the future.

CONTENTS

Introduction.....	1
1.1 Background	1
Quartz crystal microbalance (QCM).....	5
2.1 Piezoelectric effect.....	5
2.2 AT-Cut quartz crystal.....	8
2.3 QCM sensor equivalent circuits.....	10
2.4 Theoretical basis of QCM technique	13
Low-cost QCM system platform design.....	15
3.1 General QCM system	15
3.2 Arduino.....	17
3.3 Oscillator circuit	19
3.4 Interfaces for QCM system platform.....	35
Experimental.....	39
4.1 Materials.....	39
4.2 Instrumentation	39
4.3 Procedures	40
Result and discussion.....	45

5.1 Comparison of three different oscillator circuits to measure 10MHz and 6MHz QCM sensors frequencies with or no cell.	45
5.2 Morphology of TiO ₂ coating	46
5.3 Methyl orange light degradation	48
5.4 Oscillator circuit unit three applied to electrochemical test	50
5.5 Test two oscillator circuit units and difference frequency of each of both without cell.....	50
5.6 Ethanol evaporation on one QCM sensor without liquid cell	54
5.7 The study on the photocatalytic degradation processing of Rhodamine B (RB) at the Surface of nanocrystalline TiO ₂ by QCM sensor	55
Other equipment designed with Arduino microcontroller board.....	57
Conclusion	63
APPENDIX A: OSCILLATOR CIRCUIT SCHEMATIC DIAGRAM.....	65
APPENDIX B: OSCILLATOR CIRCUIT PCB BOARD SCHEMATIC DIAGRAM	66
LITERATURE CITED	68

LIST OF FIGURES

Figure 2.1.1 Piezoelectric effect in quartz crystal.....	7
Figure 2.1.2 Direct piezoelectric effect and inverse piezoelectric effect.....	8
Figure 2.2.1 Different models of cut in quartz crystal.....	9
Figure 2.2.2 Frequency change with temperature range of different models crystal.....	9
Figure 2.2.3 QCM sensor thickness shear mode of vibration.....	10
Figure 2.3.1 Quartz crystal unit and Butterworth-Van-Dyke (BVD) equivalent circuit model of QCM.....	11
Figure 3.1.1 Schematic of the QCM vibration model and the general QCM system	16
Figure 3.2.1 Arduino UNO and Arduino Mega2560.....	18
Figure 3.2.2 Shield board of oscillator circuits and flip-flops chip.....	19
Figure 3.3.1 SN74LVC1GX04 crystal oscillator driver logic diagram.....	20
Figure 3.3.2 Oscillator circuit based on SN74LVC1GX04 crystal oscillator driver.....	22
Figure 3.3.3 SN74LS74AN top view and logic diagram.....	23
Figure 3.3.4 D-type positive-edge-trigger ports.....	24
Figure 3.3.5 Difference frequency generated by D-type trigger.....	25
Figure 3.3.6 The Arduino Mega2560 before and after combing with oscillator circuit shield board.....	26
Figure 3.3.7 Schematic diagram of oscillator circuit unit two.....	27
Figure 3.3.8 Oscillator circuit unit two.....	27
Figure 3.3.9 Thermistor with 10 K Ω connect to Arduino UNO.....	28
Figure 3.3.10 Schematic diagram of oscillator circuit unit three	29
Figure 3.3.11 Power supply for oscillator circuit unit three.....	29

Figure 3.3.12 Oscillator circuit unit three and power supply circuit.....	30
Figure 3.3.13 Arduino software (IDE) for code writing.....	31
Figure 3.4.1 QCM system interface programmed by Java language.....	36
Figure 3.4.2 QCM system interface designed by Labview.....	37
Figure 3.4.3 Block diagram for Labview interface.....	37
Figure 3.4.4 Labview interface with real-time monitoring for frequency counter.....	38
Figure 3.4.5 Block diagram for interface.....	38
Figure 4.3.1 Oscillator circuit unit one with two QCM sensors	42
Figure 4.3.2 Oscillator circuit unit two with two QCM sensors.....	43
Figure 4.3.3 photocatalytic degradation processing of Rhodamine B (RB) at the Surface of nanocrystalline TiO ₂	44
Figure 5.2.1 SEM scanned features of 10mg/ml, 15V, 30s; 5mg/ml, 10V, 30s; 5mg/ml, 5V, 30s;5mg/ml, 5V, 15s; 50mg/ml, 1V, 15s; and 5mg/ml, 1V, 30s TiO ₂ electrophoretic deposition.....	47
Figure 5.3.1 Photocatalytic degradation of 6MHz methyl orange-TiO ₂ -coated QCM sensor.....	49
Figure 5.3.2 Photocatalytic degradation of 10MHz methyl orange-TiO ₂ -coated QCM sensor.....	49
Figure 5.5.1 The frequencies of two QCM sensor in unit one.....	52
Figure 5.5.2 Calculated values VS experimental values in unit one.....	52
Figure 5.5.3 The frequencies of two QCM sensor in unit two.....	53
Figure 5.5.4 Calculated values VS experimental values in unit two.....	53
Figure 5.6.1 Ethanol evaporation on one QCM sensor without liquid cell.....	55

Figure 5.7.1 Photocatalytic degradation processing of Rhodamine B (RB) at the Surface of nanocrystalline TiO ₂	56
Figure 5.7.2 Photocatalytic degradation processing of Rhodamine B (RB) at the Surface of nanocrystalline TiO ₂ -GP.....	57
Figure 6.1 Multi-channel valves array system.....	59
Figure 6.2 Logic diagram for multi-channel valves array system.....	60
Figure 6.3 Labview interface for Multi-channel valves array system.....	61
Figure 6.4 Adjustable micro-doses injection system for monolayer film formation system.....	62
Figure 6.5 Thermogravimetric analysis system with quartz crystal microbalance.....	63

LIST OF TABLES

Table 2.3.1 Parameter of Sauerbrey equation.....	13
Table 3.2.1 Technical specifications of Arduino UNO and Mega2560.....	17
Table 5.1.1 Comparison of three circuits QCM sensors frequency measured by frequency counter.....	45
Table 5.2.1 Comparison of 6MHz and 10MHz QCM sensor coating TiO ₂ film.....	48
Table 5.3.1 Comparison of 6MHz and 10MHz TiO ₂ -coated QCM sensor coating methyl orange film.....	48
Table 5.3.2 Comparison of 6MHz and 10MHz light degradation.....	49

LOW-COST QUARTZ CRYSTAL MICROBALANCE SYSTEM PLATFORM
DESIGNED FOR CHEMICAL NANOPARTICLE ANALYSIS BASED ON ARDUINO
MICROCONTROLLER BOARD

Danming Wei

August 2016

72 Pages

Directed by: Yan Cao, Bangbo Yan, and Darwin Dahl

Department of Chemistry

Western Kentucky University

QCM sensor is a response to a kind of broad spectrum, high sensitivity, and simple structure, low-cost detection device, and particularly its quality as a type of gas sensor is widely used. With the successful oscillation in liquid phase, QCM sensor has been involved in the application analytical chemistry, surface chemistry, biochemistry and environmental monitoring side and many other scientific fields. With sensitive surface film as the sensitive element, AT-cut quartz crystal as energy transducer components by changes of the relationship between mass of surface film and frequency of QCM sensor transduces signals of mass or concentration into output frequency signal of sensor, thus achieve changes of mass or concentration detection. This paper mainly states how to design a low-cost QCM system platform with Arduino microcontroller board based on QCM sensor specific properties. For the oscillator circuit selection and differential frequency circuit design, the shield board has properly matched Arduino Mega2560, then by programming code to make Arduino acquire frequency of QCM sensor in real-time. Meanwhile, the interface and data store are corresponding convenient for real-time observing and data post-processing. By the tests of anhydrous ethanol evaporation, QCM system platform was calibrated and Sauerbrey equation verification. Moreover, this paper studies that photocatalytic degradation processing of Rhodamine B (RB) and methyl orange solution at the Surface of nanocrystalline TiO_2 by QCM sensor.

Key words: QCM sensor, Arduino, frequency measurement, photocatalytic degradation

Introduction

1.1 Background

In 1880, piezoelectric effect was first discovered by French physicists Jacques and Pierre Curie¹, it brought to scientists a new direction of electromechanical interaction between electrical and mechanical state in crystalline materials with no inversion symmetry². After that, scientists began to explore electromechanical area and tried to find certain relationship between them. In 1959, German physicist Sauerbrey³ firstly was engaged in research about the relationship between mass absorption on the surface of quartz and offset of its frequency in gas phase, which established the foundation for quartz crystal microbalance(QCM) researches in various areas of sciences until now. Meanwhile, he came up with the famous Sauerbrey equation, which became the indispensable key for science to explore micro-mass world. Later, King⁴ was the first person who applied QCM sensor into chemical analysis, and a series of gas detection experiments based on QCM sensor were put in practice, and J. F. Ai de and J. J. McCallum⁵ ^{5b} made a detailed review about that. In the early gas phase analysis, there were no active materials to fix chemical compounds onto the QCM sensor surface. In 1983, Guilbault⁶ discovered dehydrogenase when methanol was for fixed on the QCM sensor surface. Certain properties of methanol could be detected by the QCM sensor. Later on, he companied with Ngeh-Ngwainbils⁷ firstly tried to investigate the immune reaction in gas phase. They coated parathion antibody on QCM sensor surface to detect the change of quinalphos.

In 1972, Shons et al⁸ developed the first piezoelectric immune sensor which combined piezoelectric sensor and immune reaction. From then on, most researchers, like Muramatsu, Guibault, Okahata, Thompson, and so on, began working on intensive researches and applications on the piezoelectric immune sensor. Now, the piezoelectric immune sensor has been applied into various areas to understand behaviors of bacteria⁹, virus^{11 12 13}, and proteins¹⁴, such as clinical diagnosis, industrial control, food and drug analysis, and environmental protection and so on.

There were two main methods in the early research on the piezoelectric biosensor: immersion and drying¹⁵. For example, the bio-active materials are attached on the piezoelectric sensor and immersed into determined solutions to react for a while, taken out for drying and weighed or measured for other changes of properties. Therefore, this dry method was more cumbersome because of many steps of cleaning and drying included, but its measurement occurred in the gas phase which was not effected by some factors in the liquid phase. In 1980, Konash and Bastiaans¹⁶ tried to design QCM sensors which could detect in liquid phase by improving the circuits to make QCM sensors vibrate more stably. In 1982, Nomura and Okuhara¹⁷ explored frequency response of QCM sensor in liquid phase, and came up with experienced equation, which correlated the change of frequency with the square root of density and viscosity of the liquid. In 1985, Kanazawa and Gordon¹⁸ came up with a theory model about the correlation between frequency response and parameters of QCM sensor and liquid. In the same year, Bruckenstein and Shay¹⁹ also gave a similar equation which was verified by experiments. At present, piezoelectric sensors mostly can be directly contact testing solutions so that it could acquire real-time data on reactions on QCM sensor surface. Usually, piezoelectric

sensor is unloaded in a flow chamber, and one side of sensor was sealed from the liquid, the other side directly contacts to the flow liquid. The tested materials are coated on the QCM sensor which could be reacted with constituents in liquid directly. However, the methods above were only limited to sensor in single channel.

The research methods of piezoelectric sensors could be divided into two types: active and passive^{20 21}. Active method is also called oscillating method, which means that sensor needs to be connected into an oscillator amplifier circuit as a part to provide positive feedback. The piezoelectric crystal would vibrate on its own frequency that could be measured by frequency counter. However, in the passive method, the piezoelectric crystal needs to be connected to measure port of instrument as an external component, like an impedance analyzer or a spectrum analyzer, which stimulates different frequency sine waves at two sides of piezoelectric crystal and records the output signals from crystal. By comparison of input and output signals, it could acquire some parameters of crystal like impedance, admittance, phase and so on. If combined electrical characteristics of equivalent circuit of piezoelectric crystal and ones of experimental environment, it could obtain relevant information by analyzing the change of parameter of crystal before and after reaction. Thus, the oscillating method has several advantages, such as simple structure, easy operation, and forming small functional instruments. But it only provided limited properties of the piezoelectric crystal in reaction environments. On the contrary, the passive method could provide multiple electrical parameters and also obtain all-sided and multi-dimension information of the piezoelectric crystal. Therefore, instruments for the passive method are complicated and expensive, and the active method has been adopted into the piezoelectric biosensor applications. Okahata et al²² employed

27 MHz QCM to research hybridization kinetics of the nucleic acid and measured relevant kinetics constant.

Most piezoelectric sensors are used mainly based on mass sensitive properties of piezoelectric material; the frequency of sensor is affected by mass absorbed on surface of the piezoelectric sensor. Thus, it is also called as the mass piezoelectric sensor. All of mass piezoelectric sensors are applied into research based on the Sauerbrey equation to measure the change of mass. However, some piezoelectric sensors are also applied into non-mass researches, such as viscosity, density, stress, viscoelasticity, conductivity, dielectric, and surface properties. Schmittl²³ adopted piezoelectric sensors to measure a variety of electricity and mechanical characteristics in liquid phase. Moreover, he discovered the best angle (AT-cut) for cutting crystal to get crystal, which is more stable under room temperature. Kanazawa²⁴ pointed out frequency response was not only affected by absorbed mass on the sensors, but also mechanical characteristics of deposition film. So he set up an electric-mechanical model to describe that mechanical characteristic of deposition film on sensors could affect sensor frequency response. This model could be applied into both steady state and transient state.

The piezoelectric material acts as a core part in the piezoelectric sensor. The acoustic wave spread acts as a method for measuring. When acoustic wave spread in piezoelectric medium, it could be influenced by property of medium, direction of cutting, and thickness. Utilizing different transducer could stimulate different kinds of acoustic waves. Acoustic waves used in biosensor included: bulk acoustic wave (BAW), surface acoustic wave (SAW)^{25 26}, acoustic plate mode (APM)^{27 28}, and love wave (LW)^{29 30}. Bulk acoustic wave was a widely pattern of acoustic waves in piezoelectric sensor

applications because it spread in the medium. It usually is made of quartz crystal cut by AT-cut as medium, acoustic wave formed standing wave by spreading in thickness direction, so the directions of particle vibration and wave spreading were vertical, which was called thickness shear mode (TSM). Therefore, sensitivity of BAW was related to thickness of crystal, the thicker it is, the more sensitive it is. QCM is a piezoelectric sensor depended on bulk acoustic wave mode. At present, QCM has been widely adopted in various areas of science because of its simple structure and high sensitivity.

Quartz crystal microbalance (QCM)

In the area of natural science research, the measurements of mass always encounter various problems. Scientists are eager to explore much smaller trace amount change of chemical compounds in reactions. The request for measurement precision is significantly taken in account, especially in nanogram level (ng). The QCM sensor technology is a new method of mass measurement to detect chemical compounds in nanogram level.

2.1 Piezoelectric effect

When a piezoelectric substance is squeezed or stretched by a mechanical stress, its surface will produce an electric charge. When the mechanical stress is taken away, the piezoelectric substance turns to a balance state and no electric charge exists. This phenomenon is called piezoelectric effect. Specifically, it is because of electric polarization when mechanical stress is applied on some certain piezoelectric substances

like crystal. This electric polarization is proportional to the strength of mechanical stress, the positive and negative of polarization is depended on the direction of stress. The electric polarization of substance formed by mechanical methods is named the piezoelectric effect, conversely, a mechanical deformation is produced when an electric field is applied, which is named the inverse piezoelectric effect. The common piezoelectric materials are classified into four categories: piezoelectric crystals, piezoelectric ceramic, macromolecular piezoelectric materials, and semiconductor materials. Among them, the piezoelectric quartz crystal has been widely applied to various scientific fields due to its excellent mechanical, electrochemical and thermal integrated properties.

Here we take quartz crystal as the example to illustrate how piezoelectric effect works, as shown in Figure 2.1.1. When no external mechanical stress, the internal potential is zero, as shown in Figure 2.1.1a. If a squeeze stress is applied in X axis lead to crystal deformation, A and B surface produces same amount of positive and negative charge respectively, as shown in Figure 2.1.1b. Conversely, if a stretch stress is applied to crystal, it forms the opposite polar charge. When the same stress is applied in Y axis, it will produce same results, as shown in Figure 2.1.1c. However, if a stress is applied in Z axis, there will be no charge formed because silicon ions and oxygen ions move in parallel translation symmetrically.

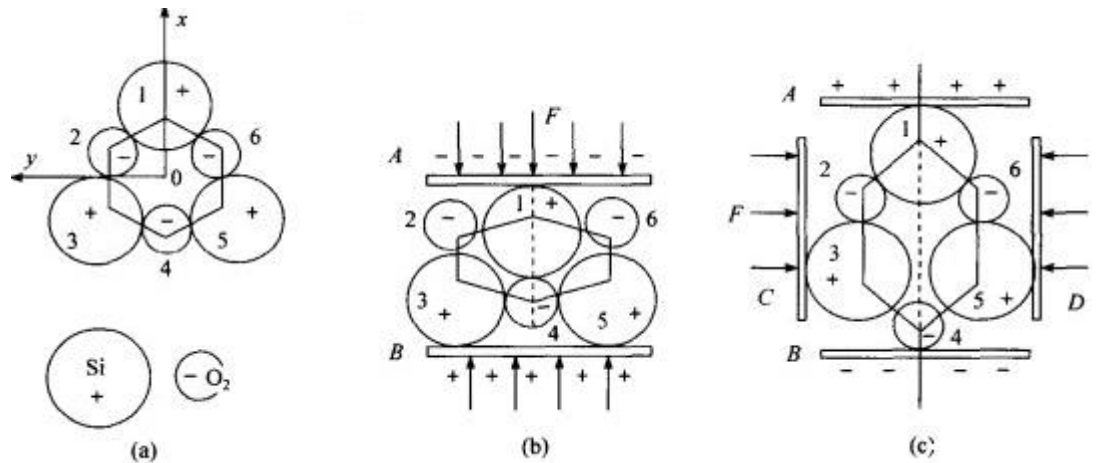


Figure 2.1.1 The piezoelectric effect in quartz crystal

Quartz crystal is an excellent piezoelectric material, when a mechanical stress (contract or elongate) is applied to it, corresponding surface will generate same amount of positive and negative charges because of deformation polarization, the direct piezoelectric effect occurs. On the contrary, the inverse piezoelectric effect occurs when an electric field is applied, crystal appears deformation in certain direction. In a certain range, there is a linear relationship between deformation of crystal and intensity of electric field. If electric field is alternative, mechanical oscillation will occur in crystal lattice, as shown in Figure 2.1.2 (F). When frequency of oscillation, inherent frequency of the quartz crystal, and frequency of oscillate circuit are same, the quartz crystal will generate most stable resonance. Under resonant status, one can obtain inherent frequency of quartz crystal by measuring frequency of oscillate circuit. The quartz crystal microbalance system is designed based on above theory, which is putting quartz resonator into oscillate circuit.

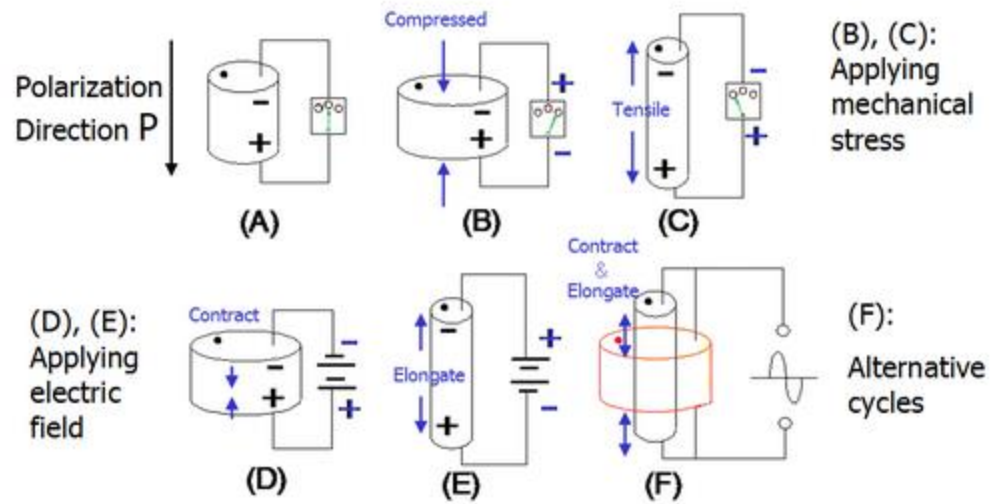


Figure 2.1.2 The direct piezoelectric effect and the inverse piezoelectric effect

2.2 AT-Cut quartz crystal

For quartz crystal, there have several models of cuts related to different modes of vibration as shown in Figure 2.2.1, for each mode of vibration there is an optimal angle of cut which controls the frequency deviation of the quartz crystal over the temperature range. From Figure 2.2.2, it demonstrates typical AT-cut quartz crystal has relatively small frequency-temperature dependence over a large temperature range between 0 and $60^{\circ}C$, for an angle of crystal cut near $\theta = 35^{\circ}15'$, the error is $\leq \pm 1 \text{ ppm}/^{\circ}C$.³¹ Typically for a QCM sensor, it has commonly been selected AT-cut quartz crystal in a tenth of one mm of thickness, because this geometry provides a stable oscillation with almost no temperature fluctuation in frequency around an ambient temperature. In most applications, the QCM sensor depends on the circular quartz crystal operating in the thickness shear mode (TSM) of vibration, where motion laterally moves to the surface³², as shown in Figure 2.2.3.

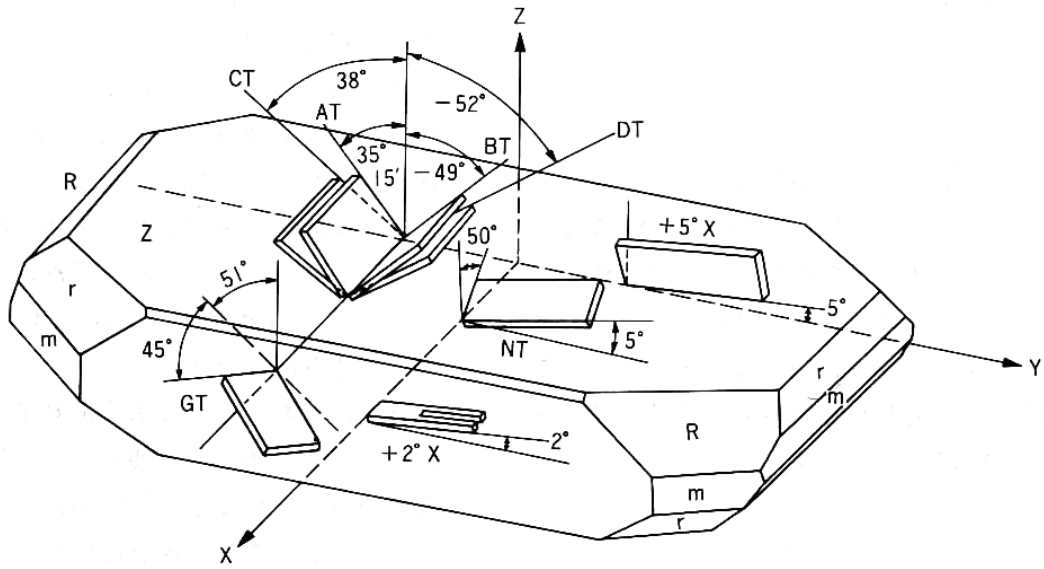


Figure 2.2.1 Different models of cut in quartz crystal

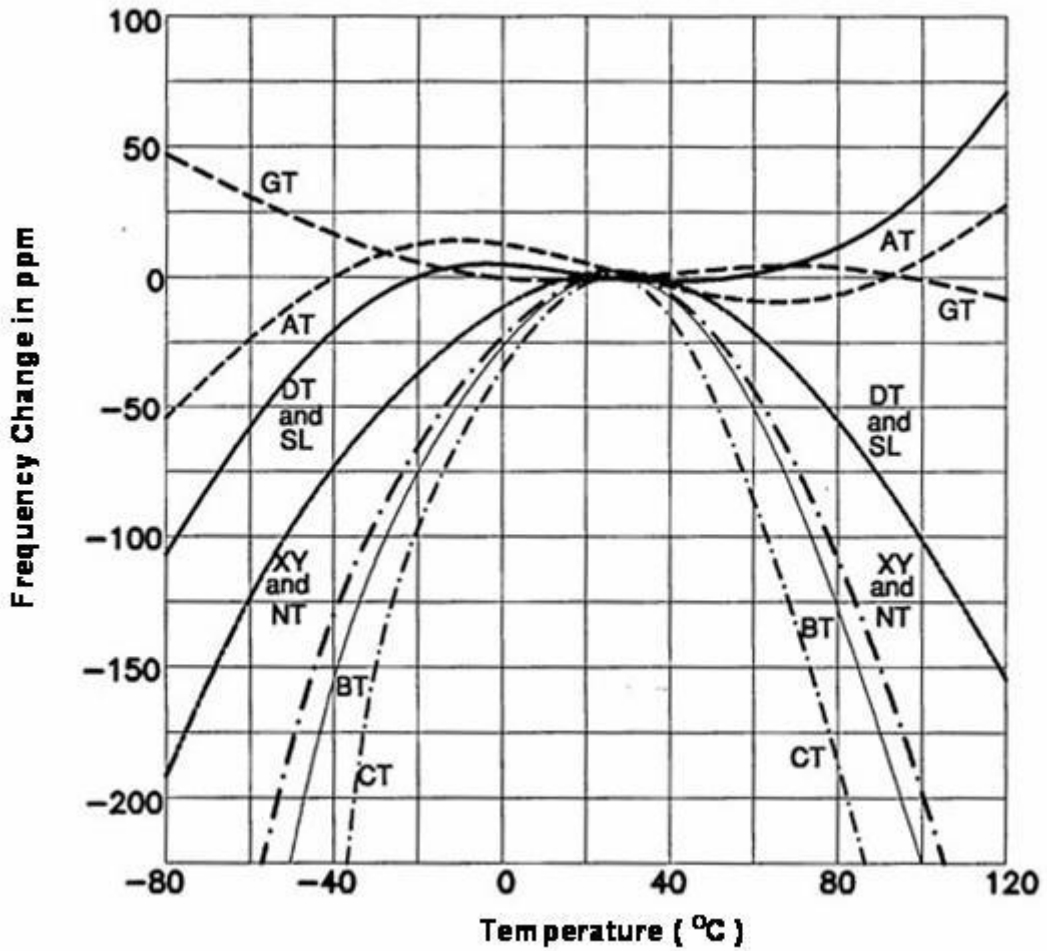


Figure 2.2.2 Frequency change with temperature range of different models crystal cut

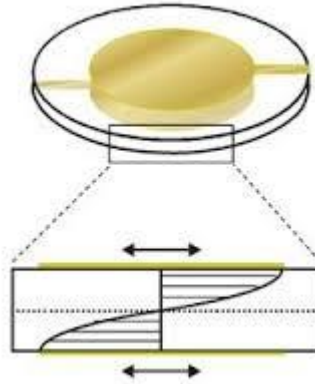


Figure 2.2.3 QCM sensor thickness shear mode of vibration

2.3 QCM sensor equivalent circuits

Generally, QCM sensor is a mass to frequency converter, which can convert tiny mass change on QCM electrode surface to change of measurable vibration frequency of QCM. Concretely, a quartz crystal unit in the main resonance frequency may be expressed as the Butterworth-Van-Dyke (BVD) model (shown in Figure 2.3.1), which ordinarily composes of the motional arm (C_1 , L_1 , and R_1) and the static arm (C_0), where X_1 is quartz crystal unit, C_1 corresponds to the dynamic capacitance (elasticity of the oscillating body), L_1 corresponds to the dynamic inductance (oscillating mass of the quartz), R_1 corresponds to the dynamic resistance (friction damping of the quartz slice, acoustic damping of ambient), and C_0 corresponds to the static parallel capacitance (capacitance between quartz electrodes).³³ C_0 , C_1 , L_1 , and R_1 are represented as following equations:

$$C_0 = \epsilon_0 \epsilon_r \frac{S}{l} \quad (1)$$

$$R_1 = \frac{l^3 r}{8SK^2} \quad (2)$$

$$L_1 = \frac{l^3 \rho}{8SK^2} \quad (3)$$

$$C_1 = \frac{8SK^2}{\pi^2 \rho c} \quad (4)$$

where ϵ_r is the relative dielectric constant, ϵ_0 is the dielectric constant in vacuum, S is the area of electrode, l is the thickness of quartz, r is the radius of quartz crystal, K is the piezoelectric stress constant, ρ is the density of quartz, and c is the wave speed in the quartz crystal.

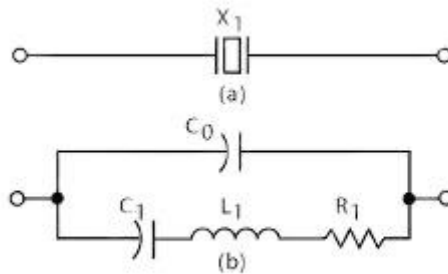


Figure 2.3.1 Quartz crystal unit and Butterworth-Van-Dyke (BVD) equivalent circuit model of QCM

From the BVD equivalent circuit, the equivalent impedance can be derived:

$$Z = \frac{R_1 + j\left(\omega L_1 - \frac{1}{\omega C_1}\right)}{1 - \omega^2 L_1 C_0 + \frac{C_0}{C_1} + j\omega R_1 C_0} \quad (5)$$

When the quartz crystal is oscillating, the equivalent impedance acts resistive, and the imaginary part is zero in equation 5, in the other word, the imaginary part of

$\left[R_1 + j\left(\omega L - \frac{1}{\omega C}\right)\right] \cdot \left[1 - \omega^2 LC_0 + \frac{C_0}{C} - j\omega R_1 C_0\right]$ is zero, which means:

$$\left(\omega L - \frac{1}{\omega C}\right) \cdot \left(1 - \omega^2 LC_0 + \frac{C_0}{C}\right) - \omega R_1^2 C_0 = 0 \quad (6)$$

Considering the value of R_1 is too small (around 100 Ohm), the R_1^2 can be ignored. So

$$\left(\omega L - \frac{1}{\omega C}\right) \cdot \left(1 - \omega^2 LC_0 + \frac{C_0}{C}\right) = 0 \quad (7)$$

Means:

$$\omega_s^2 = \frac{1}{LC} \quad \text{Or} \quad f_s = \frac{1}{2\pi\sqrt{LC}} \quad (8)$$

$$\omega_p^2 = \frac{1}{LC} + \frac{1}{LC_0} \quad \text{Or} \quad f_p = \frac{1}{2\pi} \sqrt{\frac{1}{LC} + \frac{1}{LC_0}} \quad (10)$$

Where ω_s is the series angle frequency, f_s is the series resonance frequency, ω_p is the parallel angle frequency, and f_p is the parallel resonance frequency. Because of $C_1 \ll C_0$ (C_1 value is around $10^{-2} \sim 10^{-1}$ pF, C_0 value is around several or dozens of pF), so f_s and f_p are too close. Generally thinking:

$$f = f_s = f_p = \frac{1}{2\pi} \sqrt{\frac{1}{LC}} \quad (11)$$

The equivalent circuit components of C_1 , L_1 , and R_1 are represented the mechanical properties of the quartz crystal, in parallel with a static capacitance C_0 which represents the electrical connections to the crystal. The series components determine the basic frequency of the quartz crystal oscillation which operates towards its series resonance. Quartz resonators are characterized by the following essential properties:³³

- Very high quality ($Q = 10^4$ - 10^5)
- High L/C ratio
- $C_1 \ll C_0$
- Frequency stability $\Delta f / f_{res} \leq 10^{-4}$ - 10^{-10}

2.4 Theoretical basis of QCM technique

Since 1959, Sauerbrey³ firstly discovered the proportional relationship between mass increasing on the quartz crystal surface and frequency decreasing of it accordingly. He came up with the well- known linear Sauerbrey equation (eq. 1), which found a new method to explore the micro-world. The Sauerbrey equation is used to precisely quantify, with nanogram level sensitivity, the elastic mass added to the surface of quartz crystal.³² When a QCM sensor was chosen the f_0 , ρ_q , μ_q , and A are constant, so there exists a linear proportional relationship between Δf and Δm .

$$\Delta f = - \frac{2f_0^2}{A\sqrt{\rho_q\mu_q}} \Delta m \quad (12)$$

Table 2.3.1 Parameters in the Sauerbrey equation

Δf	the measured resonant frequency change (Hz)
f_0	the intrinsic frequency of the quartz crystal (Hz)
A	the piezoelectlyrical active crystal area (electrodes)

	area, cm ²)
ρ_q	the density of quartz (2.643 g/cm ³)
μ_q	the shear modulus of quartz for the AT-cut crystal (2.947×10 ¹¹ g/cm·s ²)
Δm	the elastic mass change (g)

For example, if a $f_0 = 6.015\text{MHz}$, $A = 6\text{ mm}$ QCM sensor, the equation 12 can be turned into the equation 13. In the other word, for this QCM sensor, when the elastic mass changes in 3.4ng/cm^2 , the frequency changes in 1 Hz. But for a $f_0 = 10.015\text{MHz}$, when the elastic mass changes in 1.24ng/cm^2 , the frequency changes in 1 Hz.

$$\Delta f = -2.26 \times 10^{-6} f_0^2 \frac{\Delta m}{A} = -C\Delta m \quad (13)$$

The Sauerbrey equation was derived in vacuum or gas phase and had already been successful proved as accurate scientific approaches on mass change measurement. However, it is valid only if three conditions can be met: 1) the coated mass must be rigid film, 2) the coated mass must be distributed evenly, and 3) the change of frequency is less than 2%, which means $\Delta f / f < 0.02$.³⁴ Others added one more restriction: the mass added on QCM sensor surface must be not greater than 10% of QCM sensor mass.³⁵

After decades, research on the QCM sensor has been redirected to the liquid phase. Numerous experiments had illustrated the capabilities of the QCM sensor for measuring mass change occurring at one of the QCM electrodes being immersed into a liquid.³⁶ In the liquid phase, the resonant frequency of the QCM sensor is also affected by the viscosity and density of the liquid, because the surface of the quartz resonator was at an antinode of the shear wave generated by crystal vibration.³⁷ Fortunately, in 1985, Kanazawa and Gordon¹⁸ assumed that quartz crystal was elastic solid without loss

and liquid was a Newtonian fluid. Under this assumption, they discovered the relationship between the resonant frequency change and the viscosity and density of liquid, as follow:

$$\Delta f = -f_0^{3/2} (\rho_l \eta_l / \pi \mu_q \rho_q)^{1/2} \quad (14)$$

Where ρ_l is the density of the liquid and η_l is the viscosity of the liquid. When the QCM sensor vibrates in the liquid, the total frequency decrease cannot be deconvoluted into a contribution from a bound mass distinguishable from the liquid contribution.³² When f_0 , ρ_q , and μ_q are constant, Δf is proportional to $(\rho_l \eta_l)^{1/2}$.

Low-cost QCM system platform design

3.1 General QCM system

In order to measure the frequency of QCM sensor, based on its properties, the QCM system generally consists of 1) oscillator circuit (obtaining stable frequency signal of the QCM sensor, under the resonance frequency), 2) a frequency counter (measuring the frequency signal of the QCM sensor), 3) software (monitoring the frequency signal processing, save data, and controlling QCM system), and 4) power supply (providing power for the QCM system) as shown in Figure 3.1.1b

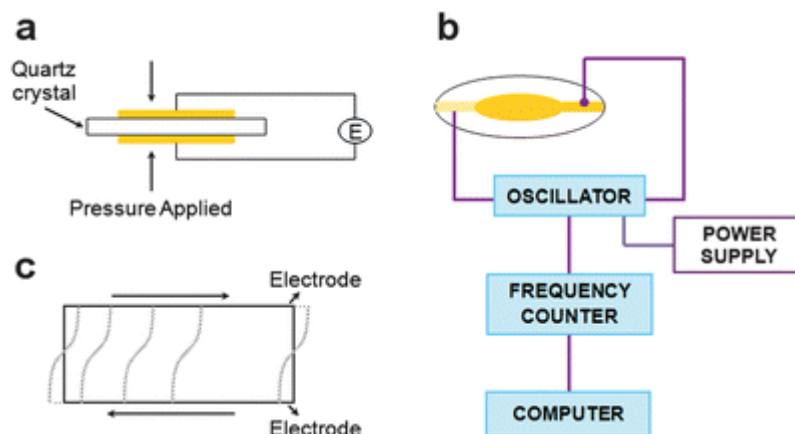


Figure 3.1.1 Schematic of the QCM vibration model and the general QCM system

The microcontroller becomes the first priority in the design of a low-cost platform for measuring the QCM frequency. Microcontroller provides a very flexible way of controlling experiments, acquiring data, and interfacing instruments to personal computers, and also offers the analytical chemist a powerful and inexpensive means of interfacing to computers and laboratory equipment³⁸.

The Arduino is a quite popular commercial open-source microcontroller board, which has recently been applied into various areas based on its powerful functions, easy programming, and low cost. Therefore, the Arduino microcontroller board has been employed as the core electrical component in our designed QCM system platform. Two practical and functional oscillator circuit boards have also been designed; one is CMOS (complementary Metal Oxide Semiconductor) oscillator circuit, the other is TTL (Transistor-Transistor Logic) oscillator circuit. The interface programming has been applied two methods including the Java language programming and the Labview programming.

3.2 Arduino

According to the Arduino official website: “Arduino is an open-source prototyping platform based on easy-to-use hardware and software, it can sense the environment by receiving input from a variety of sensors and can affect its surroundings by controlling lights, motors, and actuators.” The two common models boards of the Arduino microcontroller boards are Arduino UNO and Arduino Mega2560, as shown in Figure 3.2.1 and their technical specifications have been summarized in Table 3.2.1.

Table 3.2.1 Technical specifications of Arduino UNO and Mega2560

Arduino model	Arduino UNO	Arduino Mega2560
Microcontroller	ATmega328P	ATmega2560
Operating Voltage	5V	5V
Input Voltage(recommended)	7-12V	7-12V
Input Voltage(limit)	6-20V	6-20V
Digital I/O Pins	14 (of which 6 provide PWM output)	54 (of which 15 provide PWM output)
PWM Digital I/O Pins	6	54
Analog Input Pins	6	16
DC Current per I/O Pin	20 mA	20 mA
DC Current for 3.3V Pin	50 mA	50 mA
Flash Memory	32 KB (ATmega328P)of which 0.5 KB used by bootloader	256 (ATmega2560)KB of which 8 KB used by bootloader
SRAM	2 KB (ATmega328P)	8 KB (ATmega2560)
EEPROM	1 KB (AT mega328P)	4 KB (ATmega2560)
Clock Speed	16 MHz	16 MHz

Length	68.6 mm	101.52 mm
Width	53.4 mm	53.3 mm
Weight	25 g	37 g

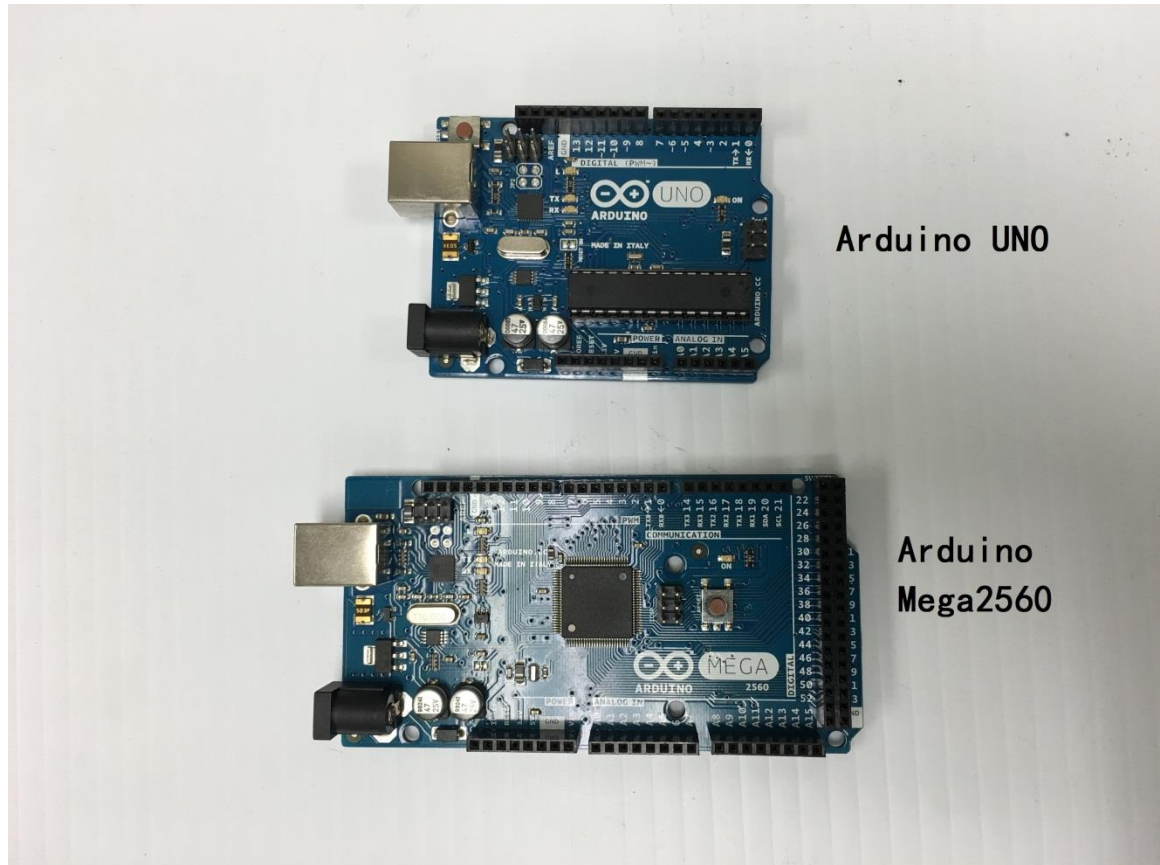


Figure 3.2.1 Arduino UNO and Arduino Mega2560

From Table 3.2.1, it is obvious that Arduino UNO and Mega 2560 are similar in function, but the number of pins of Arduino Mega2560 is much more than ones of Arduino UNO. Thus, Arduino Mega2560 can be expanded to control much more applications, such as simultaneously controlling several stepper motors, acquiring data from various sensors, and interfacing instruments to computers. These advantages bring Arduino Mega2560 to be the core component of our QCM system platform. For the

specific applications, users usually design their own shield board as the integrated circuit matched to the Arduino microcontroller board. Therefore, a shield board of the CMOS oscillator circuit has been designed for connecting the QCM sensors and stabilizing their resonance frequency, as shown in Figure 3.2.2.

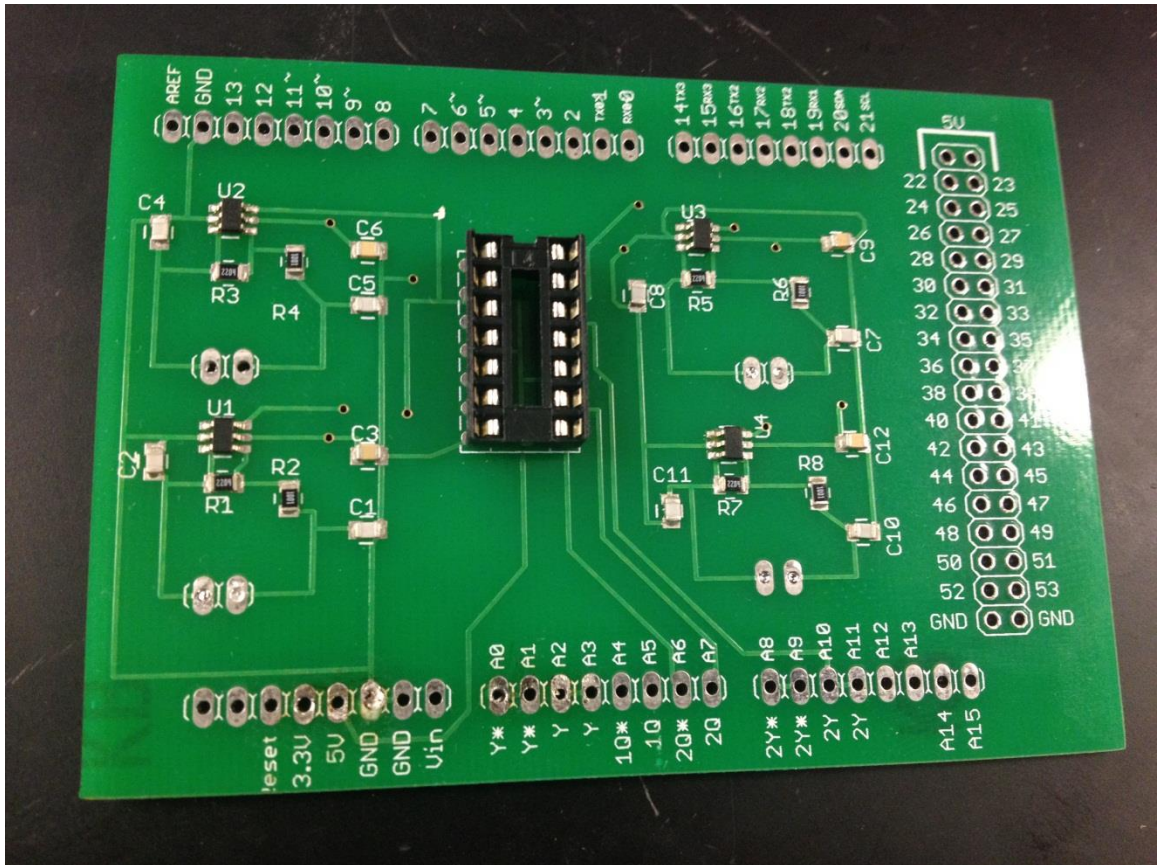


Figure 3.2.2 Shield board of oscillator circuits and flip-flops chip

3.3 Oscillator circuit

In order to measure the series frequency of QCM sensor, there are three oscillator circuit units designed for our QCM system platform. Unit one is based on the CMOS oscillator theory, which makes the crystal oscillates at its series resonance frequency. The CMOS inverter is initially biased into the middle of its operating region by the high

feedback resistor, usually more than 1 M Ω ; additional inverter is used to buffer the output from the oscillator to the connected load. The inverter provides 180⁰ of phase shift and the crystal capacitor network the additional 180⁰ required for oscillation. The advantage of the CMOS crystal oscillator is that it will always automatically readjust itself to maintain this 360⁰ phase shift for oscillation. According to the CMOS oscillator theory, SN74LVC1GX04 crystal oscillator driver is chosen to be the core component in the oscillator circuit unit one. Its top view and logic diagram are shown in Figure 3.3.1. Therefore, a modified CMOS oscillator circuit is designed with SN74LVC1GX04 crystal oscillator drivers and SN74LS74AN dual D-type positive-edge-triggered flip-flops, which is employed for generating a differential frequency of two QCM sensors, as shown in the APPENDIX A. Figure 3.3.2 shows one of four oscillator circuits based on SN74LVC1GX04 crystal oscillator driver. The whole circuit schematic diagram and PCB are designed and drawn by the Eagle software, as shown in the APPENDIX B. The PCBs are printed and made in the SeeedStudio Company, and the devices for components soldered are provided by the Department of Engineering in Western Kentucky University.

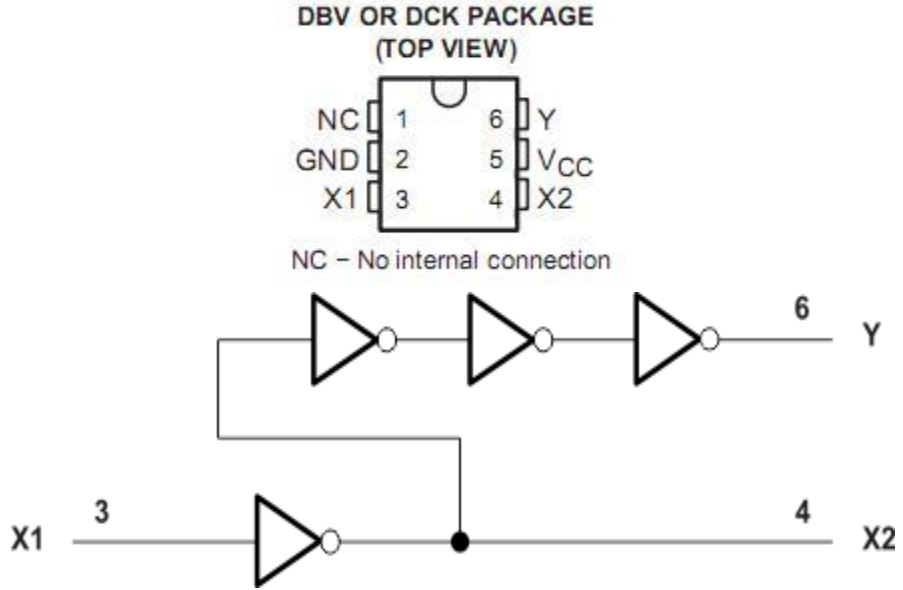


Figure 3.3.1 SN74LVC1GX04 crystal oscillator driver logic diagram

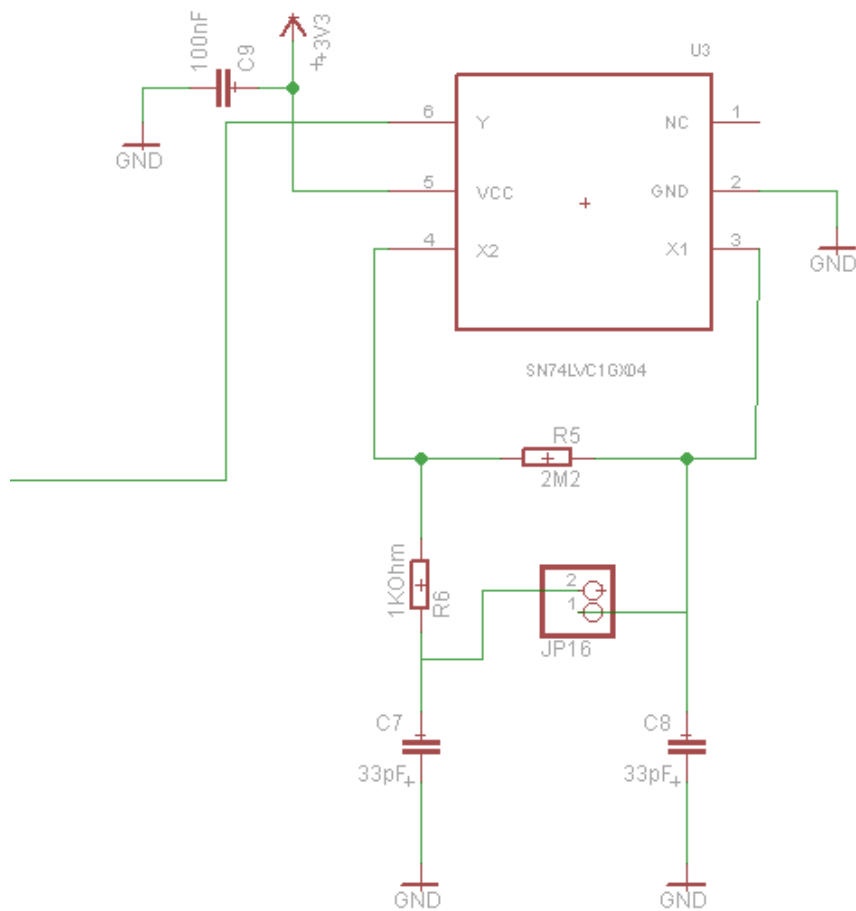


Figure 3.3.2 Oscillator circuit based on SN74LVC1Gx04 crystal oscillator driver

SN74LS74AN dual D-type positive-edge-triggered flip-flops (shown in Figure 3.3.3) are chosen for generating the difference frequency of two QCM sensors (sensing QCM and reference QCM). Because QCM sensor is so sensitive that it is affected by external environment, like temperature, especially in liquid phase, such as liquid viscosity,

density, and conductivity. In order to minimize the effects of these irresistible factors, the difference frequency should be measured during the experiments.

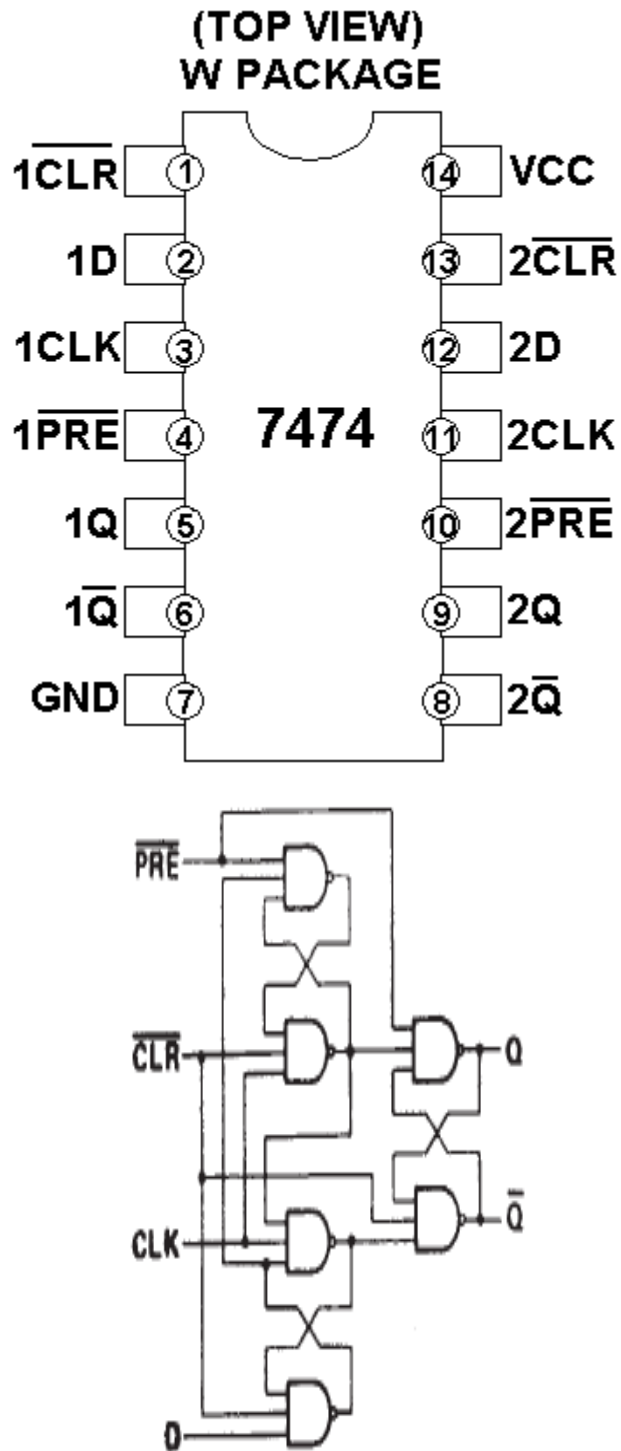


Figure 3.3.3 SN74LS74AN top view and logic diagram

Difference frequency generation theory based on SN74LS74AN satisfies following conditions: there are two frequency input signal to D port and CLK port respectively, which meets: $2/3f_{in} < f_{ck} < f_{in}$, so $f_{out} = f_{in} - f_{ck}$, shown in Figure 3.3.4.

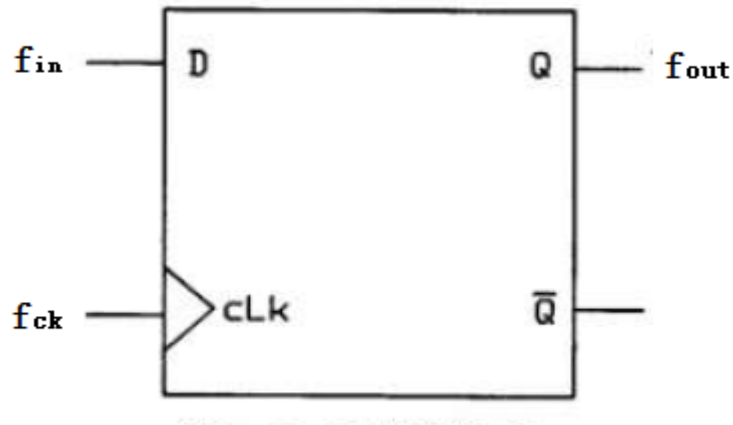


Figure 3.3.4 D-type positive-edge-trigger ports

The reference QCM frequency signal goes through D port and the sensing QCM frequency signal goes through CLK port, due to these two closed frequency, the f_{in} is a little more than f_{ck} , in each T_{ck} period, there is ΔT between T_{in} and T_{ck} . After N period of T_{in} , f_{ck} is less one cycle than f_{in} , D-trigger generate a different period signal T_0 . It is resulted: $N \cdot \Delta T = T_{ck}$, $T_0 = N \cdot T_{in}$, then $T_0 = (T_{in} \cdot T_{ck}) / \Delta T = (T_{in} \cdot T_{ck}) / (T_{ck} - T_{in})$, so $f_{out} = f_{in} - f_{ck}$ (shown in Figure 3.3.5). In the experimental section, the D-trigger function has been proved well.

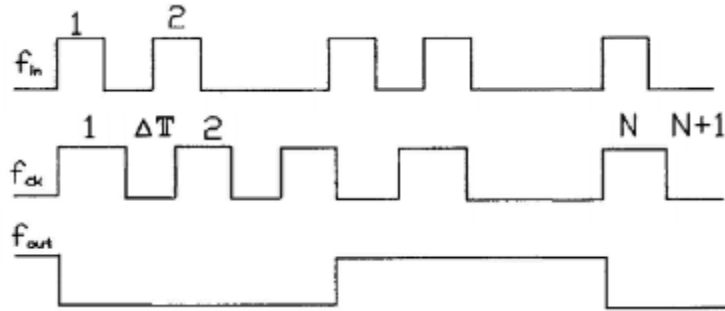


Figure 3.3.5 Difference frequency generated by D-type trigger

After soldering all resistors, capacitors, and oscillator drivers, and also soldering all pins and the holder for flip-flops, the assembly of the final product with combining Arduino Mega2560 and the shield board is shown in Figure 3.3.6. On the shield PCB, pins are also added at the same position of Arduino Mega2560 board so that the function of Arduino Mega2560 can be maintained and used.

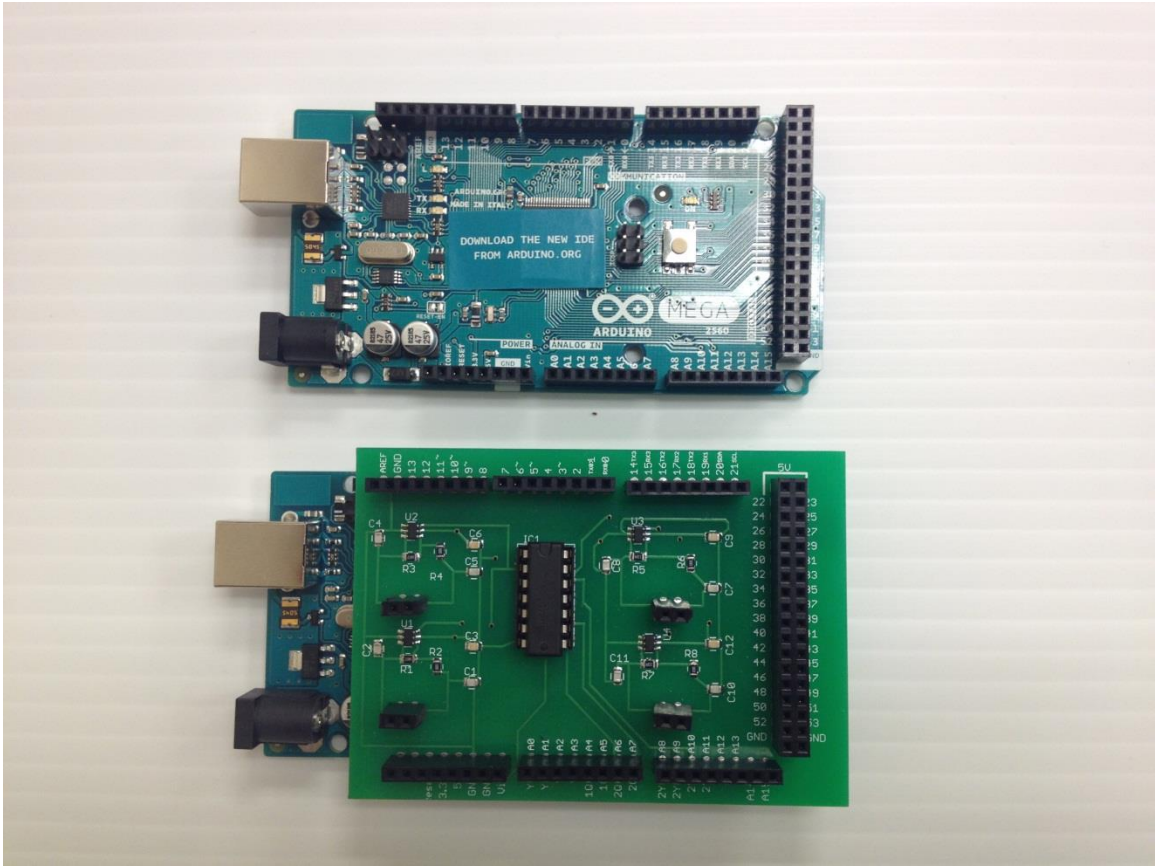


Figure 3.3.6 The Arduino Mega2560 before and after combing with oscillator circuit shield board

Oscillator circuit unit two has been designed based on TTL oscillator theory, which is designed using SN7404AN Hex Inverter to measure the series frequency of QCM sensor; the inverter performs an 180° phase shift in a series resonant oscillator circuit. Schematic diagram of oscillator circuit unit two is drawn by NI Multisim software, shown in Figure 3.3.7, where XFC is frequency counter.

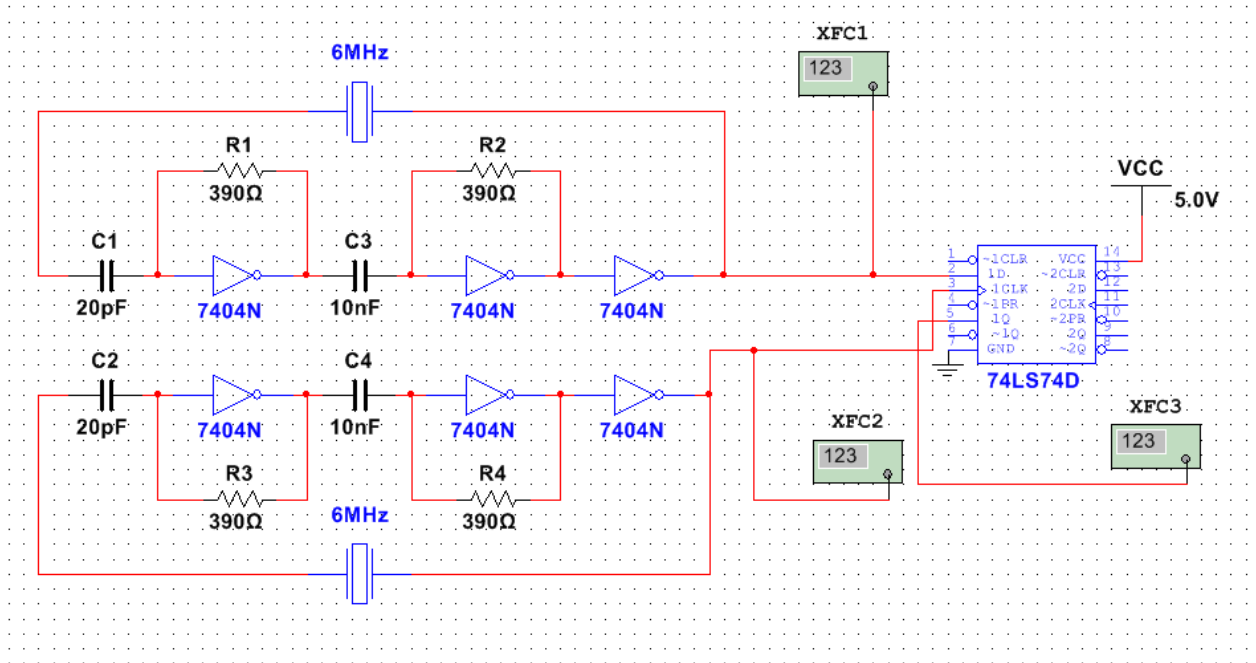


Figure 3.3.7 Schematic diagram of oscillator circuit unit two

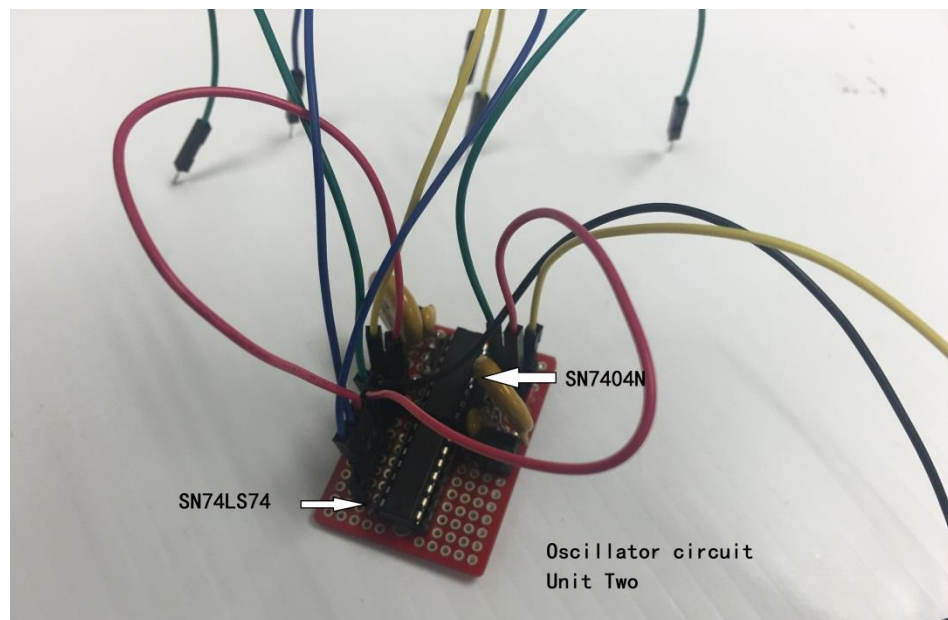


Figure 3.3.8 Oscillator circuit unit two

In order to monitor the ambient temperature during the experiment, a thermistor, which bought from Sparkfun, combining with 10 K Ω resistor, has been added into the platform, and the code has been written to measuring real-time temperature.

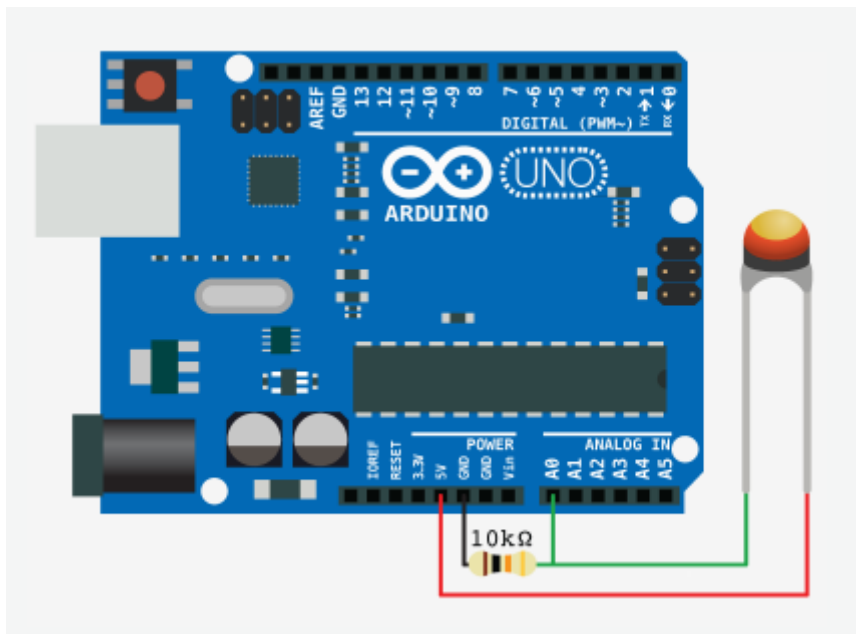


Figure 3.3.9 Thermistor with 10 K Ω connect to Arduino UNO

For the electrochemistry application, QCM sensor has to be applied into liquid phase. It requires the oscillator circuit a little more particular than the other two regular circuits. In electrochemical experiments, one electrode which is contacted to the solution works as working electrode in electrochemical system. Due to the alternating voltage running through two electrodes of QCM sensor when it is working, it is significant to make the working electrode and the electrode contacted to solution works as the same step. To figure out this problem, the oscillator circuit has been designed with one electrode of QCM sensor connecting the ground, and the potentiostat of electrochemical station is of the stand Wenking design, using a true ground for the working electrode³⁹. The oscillator circuit unit three is designed as shown in Figure 3.3.10.

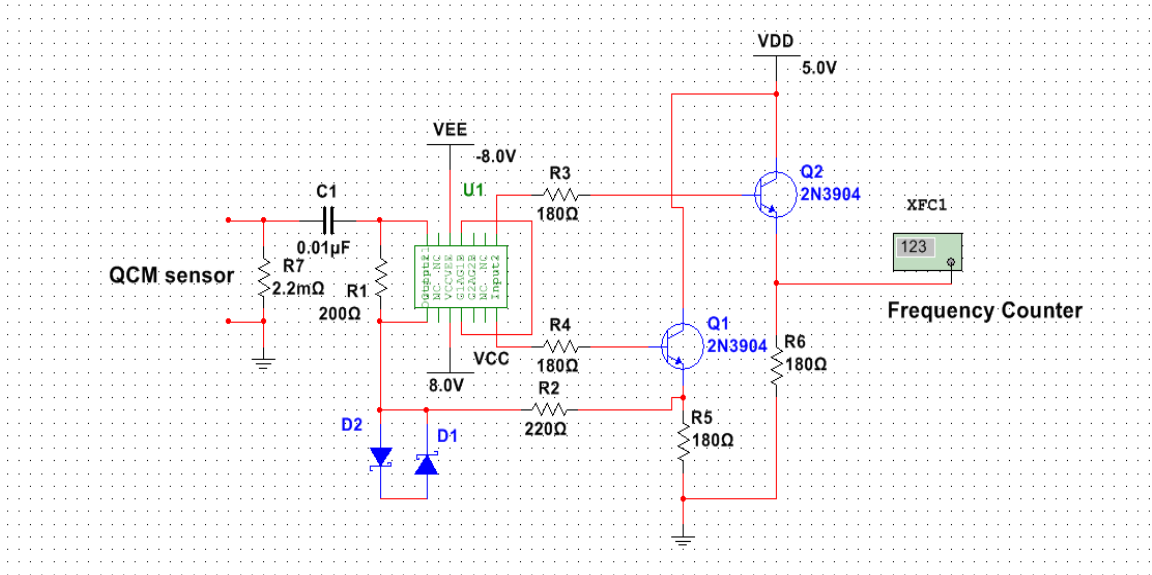


Figure 3.3.10 Schematic diagram of oscillator circuit unit three

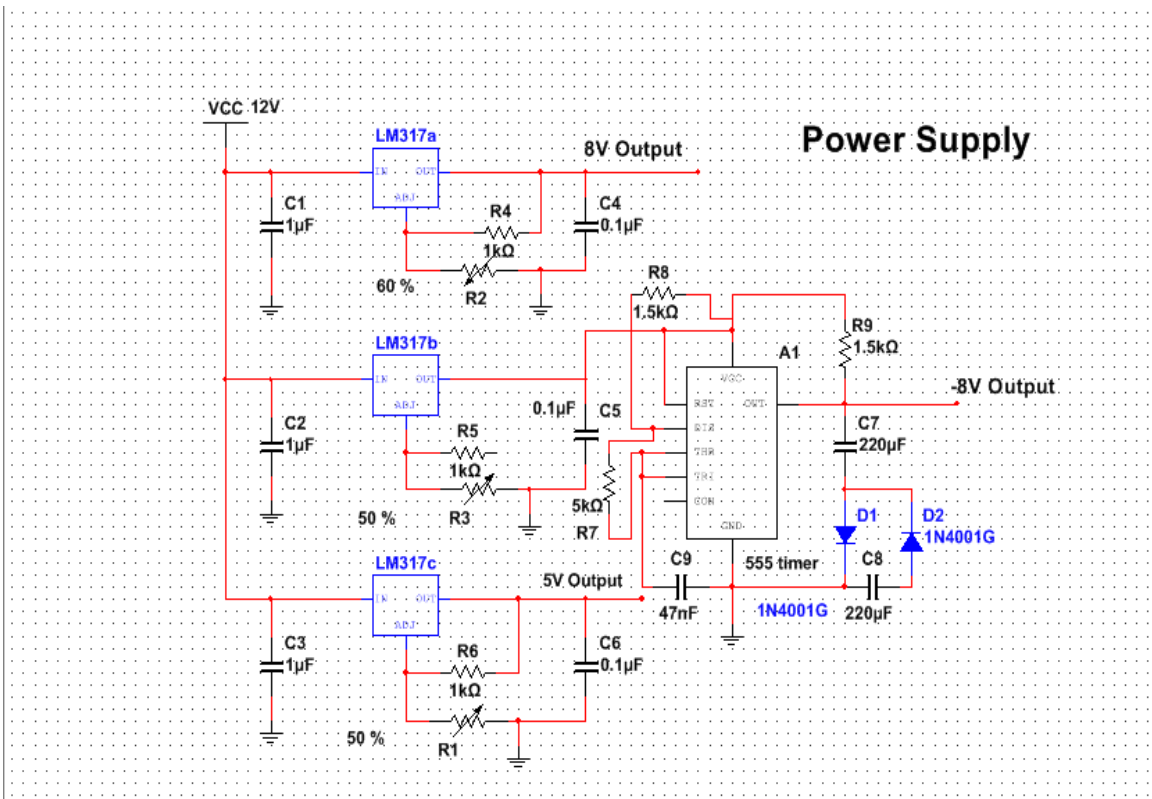


Figure 3.3.11 Power supply for oscillator circuit unit three

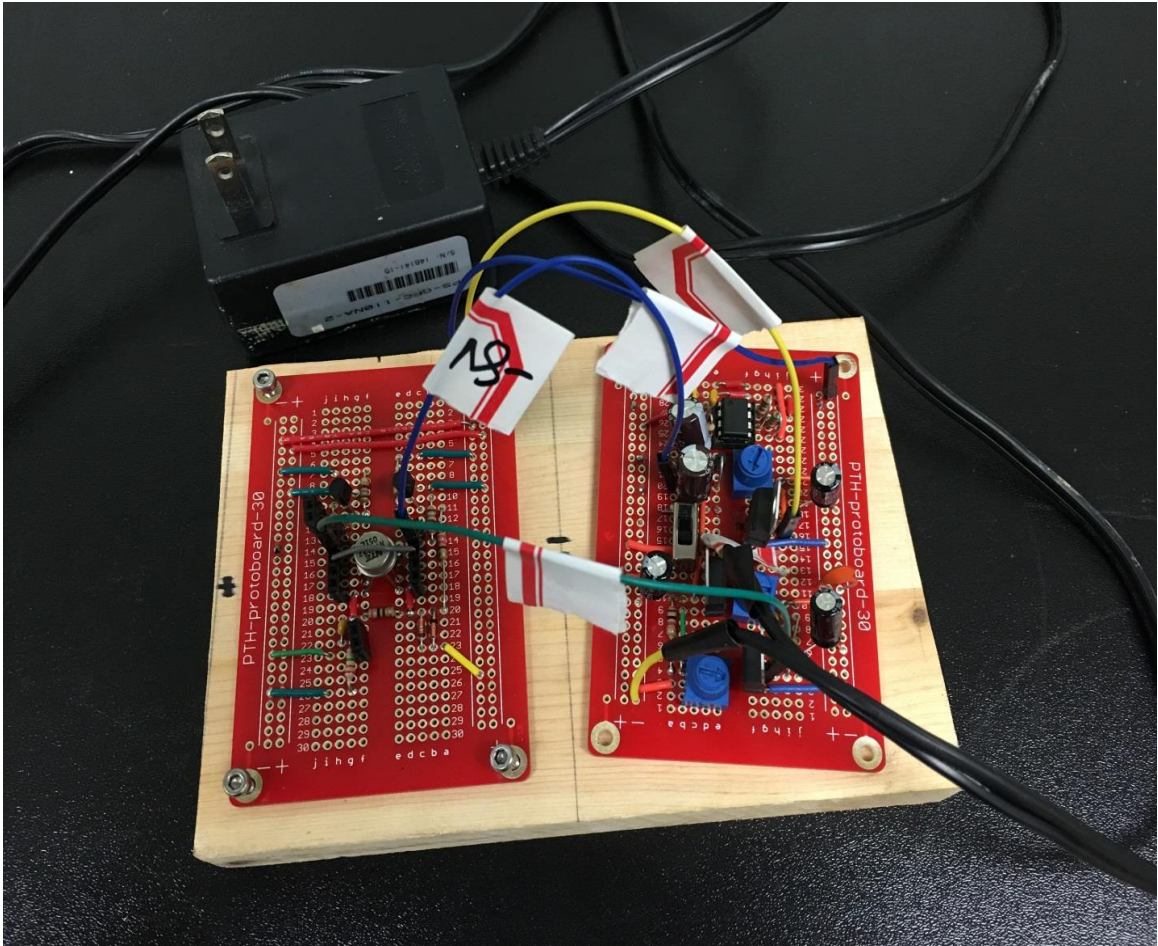


Figure 3.3.12 Oscillator circuit unit three and power supply circuit

The Arduino microcontroller board should be coding with programming languages that derive from C language, which has made Arduino board attractive for interfacing scientific equipment to personal computers. The open-source Arduino software (IDE) (shown in Figure3.3.10) is easy to write code and sketch it into the Arduino board. It can be run in Windows, Mac OSX, and Linux. The environment is written in Java and based on Processing and other open-source software.

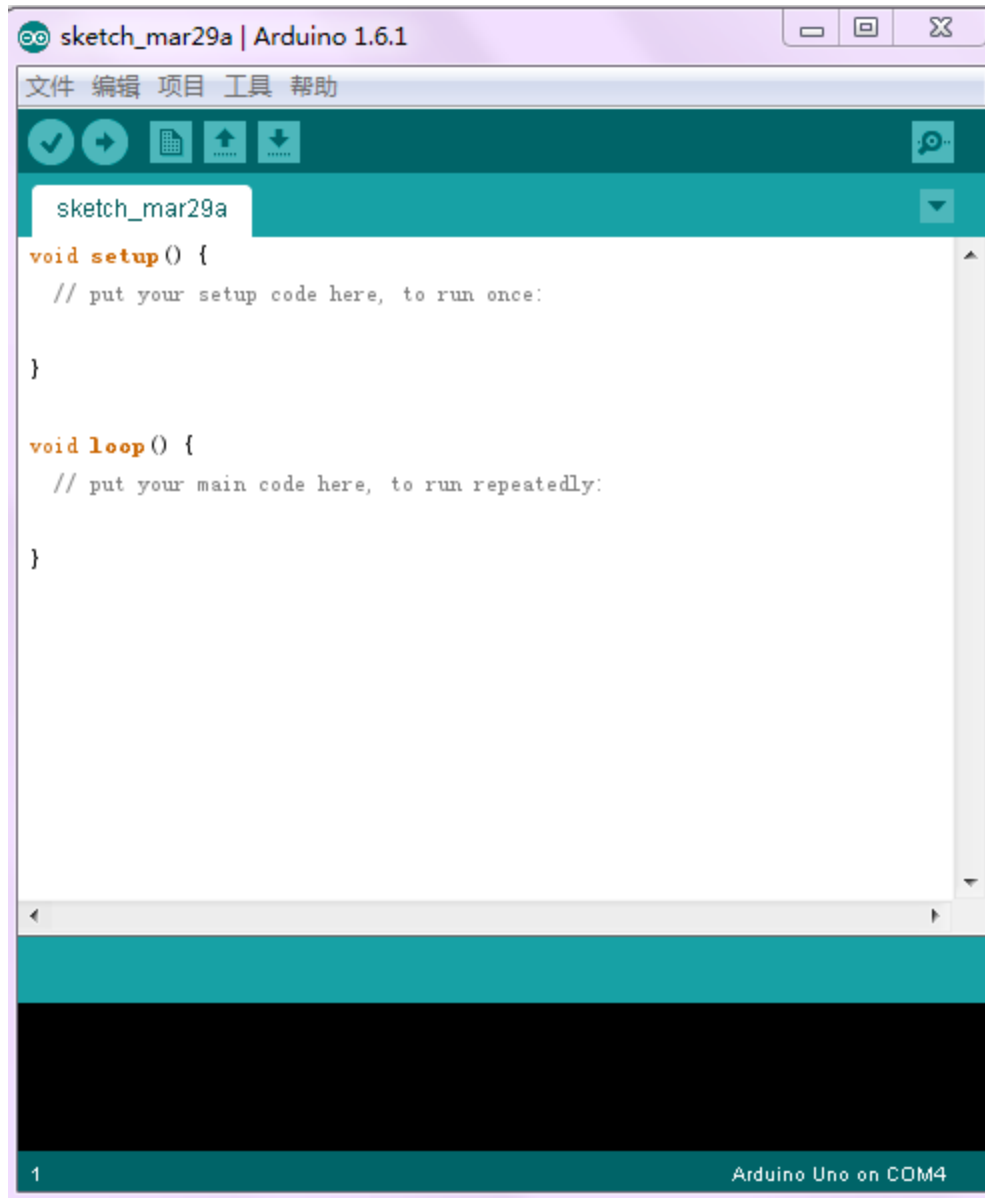


Figure 3.3.13 Arduino software (IDE) for code writing

The Arduino code has been written for measuring QCM frequency from QCM platform designed above, as shown below:

```
#include <FreqCount.h>  
  
// fixed "gate interval" time for counting cycles 1000ms  
  
#define GATE 1000
```

```
// Thermistor pin

#define THERMISTORPIN A1

// // resistance at 25 degrees C

#define THERMISTORNOMINAL 10000

// temp. for nominal resistance (almost always 25 C)

#define TEMPERATURENOMINAL 25

// how many samples to take and average

#define NUMSAMPLES 10

// The beta coefficient of the thermistor (usually 3000-4000)

#define BCOEFFICIENT 3950

// the value of the 'other' resistor

#define SERIESRESISTOR 10000

// print data to serial port

void dataPrint(unsigned long Count, int Temperature){

  Serial.print("RAWMONITOR");

  Serial.print(Count);

  Serial.print("_");

  Serial.print(Temperature);

  Serial.write(255);

}

// measure temperature
```

```

int getTemperature(void){
    int i;
    float average;
    int samples[NUMSAMPLES];
    float thermistorResistance;
    int Temperature;

    // acquire N samples
    for (i=0; i< NUMSAMPLES; i++) {
        samples[i] = analogRead(THERMISTORPIN);
        delay(10);
    }

    // average all the samples out
    average = 0;
    for (i=0; i< NUMSAMPLES; i++) {
        average += samples[i];
    }
    average /= NUMSAMPLES;

    // convert the value to resistance
    thermistorResistance = average * SERIESRESISTOR / (1023 - average);

```

```

float steinhart;

steinhart = thermistorResistance / THERMISTORNOMINAL;    // (R/Ro)

steinhart = log(steinhart);          // ln(R/Ro)

steinhart /= BCOEFFICIENT;          // 1/B * ln(R/Ro)

steinhart += 1.0 / (TEMPERATURENOMINAL + 273.15); // + (1/To)

steinhart = 1.0 / steinhart;        // Invert

steinhart -= 273.15;                // convert to C

// decimal value

Temperature = steinhart * 10;

return(Temperature);

}

// variable declaration

// QCM frequency

unsigned long frequency = 0;

// counting the number of pulses in a fixed time

unsigned long count = 0;

// thermistor temperature

int temperature = 0;

void setup(){

Serial.begin(115200);

```

```

// Configure the reference voltage used for analog input
analogReference(EXTERNAL);

// init the frequency counter
FreqCount.begin(GATE);
}

void loop(){
if (FreqCount.available())
{
count = FreqCount.read();    // counting the number of pulses

frequency = count; // measure QCM frequency

temperature = getTemperature(); // measure temperature

dataPrint(frequency, temperature); // print data
}
}

```

3.4 Interfaces for QCM system platform

Data TX (transmit) and RX (receive) between QCM system platform and personal computer is by serial communication, like USB port. So QCM system interface could be designed by some software which uses serial communication to connect external equipment. There were two interfaces employed to indicate how the change of QCM sensor frequency by time. One was being programmed by Java language, as shown in Figure 3.4.1. The other was being designed by Labview (Laboratory Virtual Instrument

Engineering Workbench) (as shown in Figure 3.4.2), which is a system-design platform and development environment for a visual programming language from National Instruments Company.

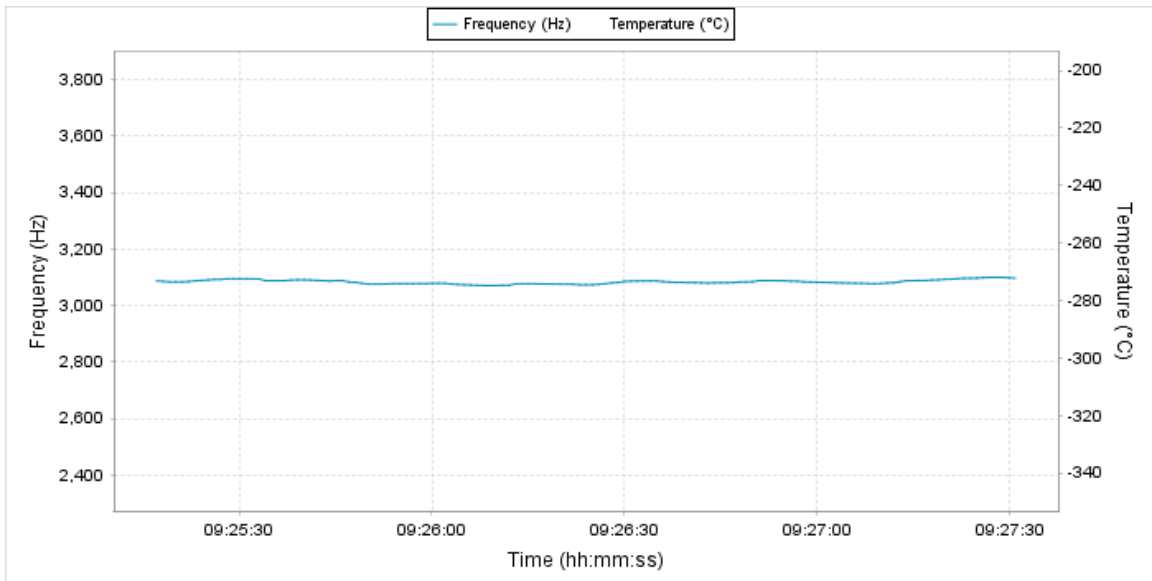


Figure 3.4.1 QCM system interface programmed by Java language

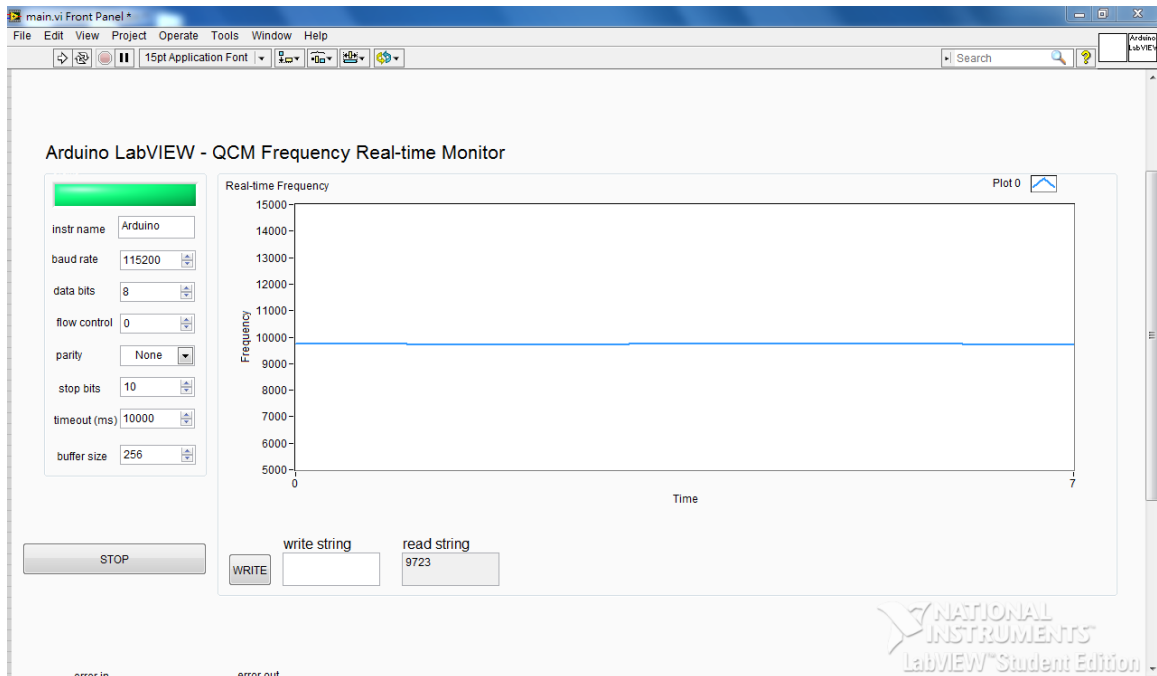


Figure 3.4.2 QCM system interface designed by Labview

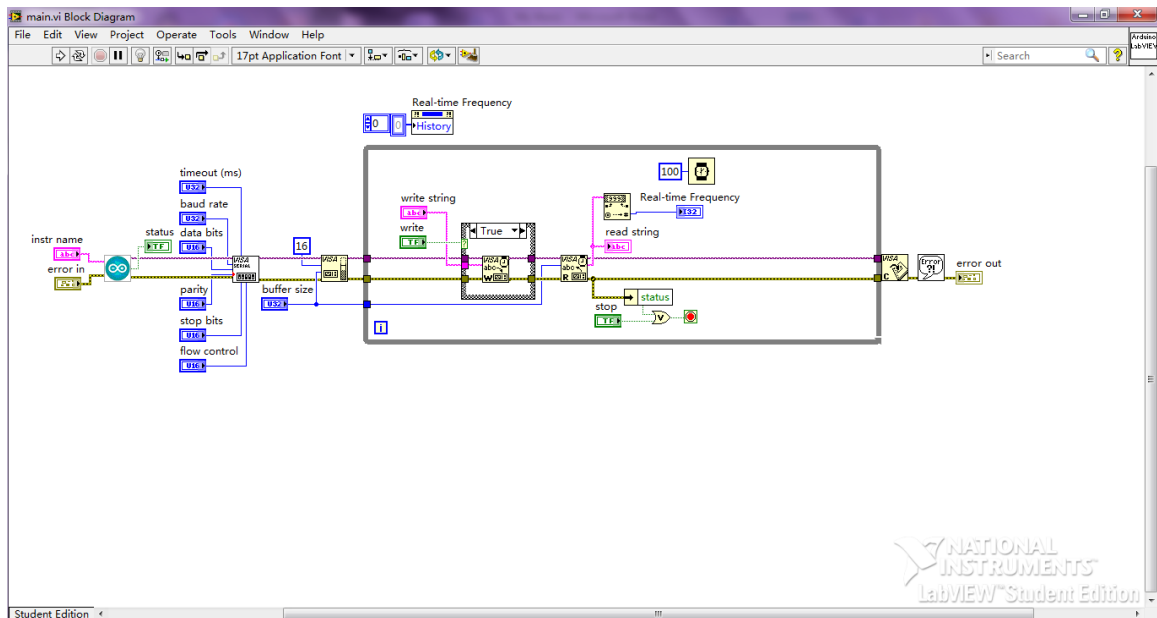


Figure 3.4.3 Block diagram for Labview interface

Due to the limitation of Arduino microcontroller board, a commercial frequency counter is also employed in the experiment. Meanwhile, the frequency counter has its

own interface programming by Labview, but some new functions like graph for real-time monitoring has been added in for experimental need (shown in Figure 3.4.4 and Figure 3.4.5).

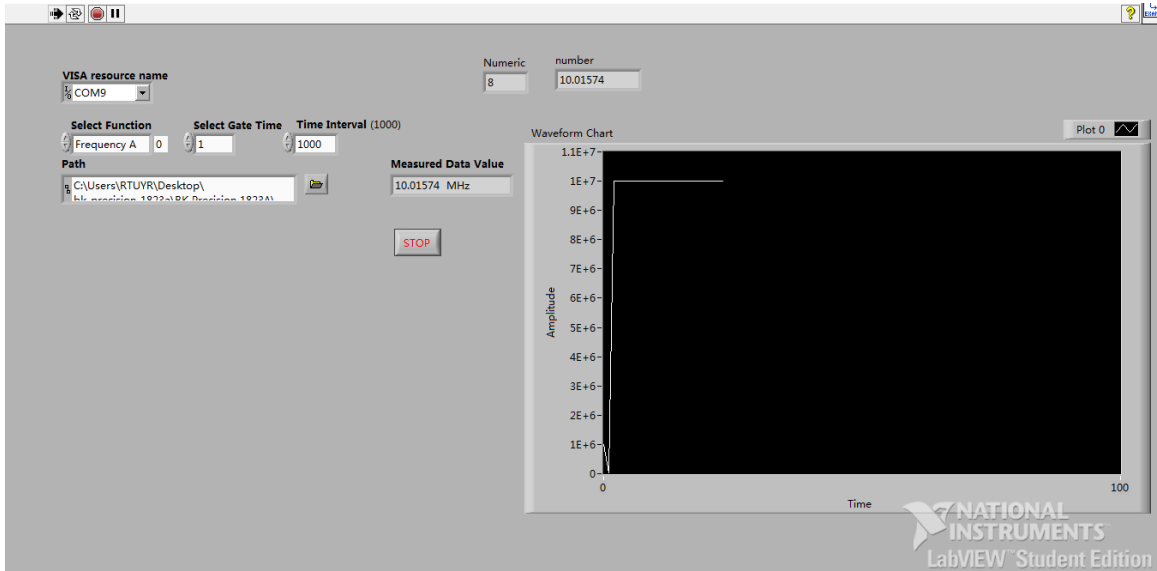


Figure 3.4.4 Labview interface with real-time monitoring for frequency counter

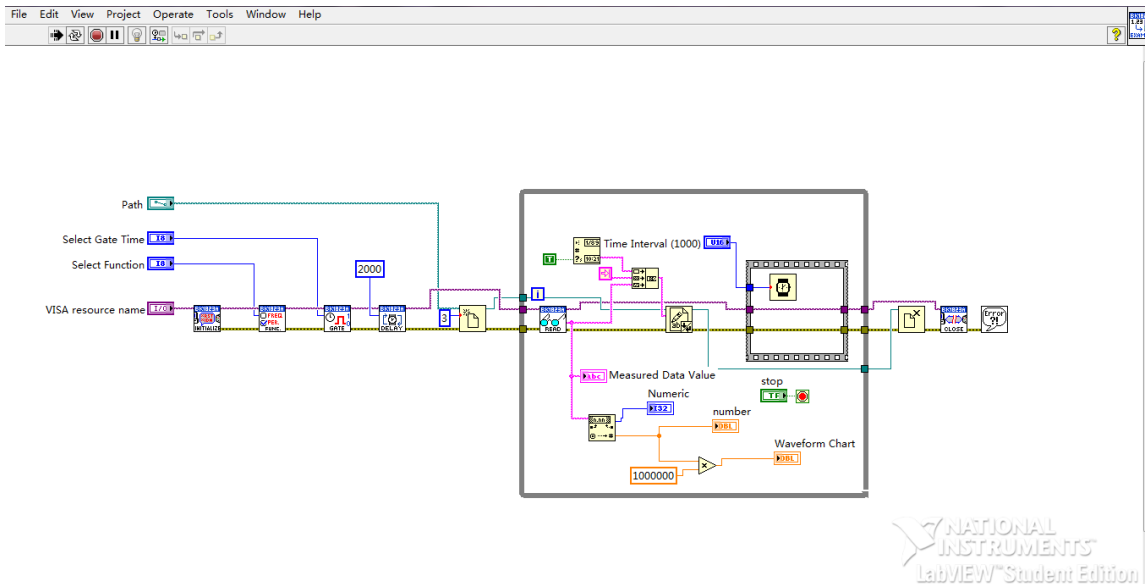


Figure 3.4.5 Block diagram for interface

Experimental

4.1 Materials

Anhydrous ethanol and acetone were chosen for evaporation experiments, which calibrate the QCM system platform whether satisfy the Sauerbrey equation. Commercial titanium dioxide powder (Evonik AEROXIDE P25) and methanol were chosen for making TiO₂ suspension to electrophoretic deposition on the surface of QCM sensor electrode. Methyl Orange was prepared for thin film photocatalytic degradation. Rhodamine B (RB) and titanium dioxide (TiO₂) were selected for the study on the photocatalytic degradation processing of Rhodamine B (RB) at the Surface of nanocrystalline TiO₂. Sodium perchlorate, sodium iodide, and sodium bromide were prepared for halide adsorption and desorption.

4.2 Instrumentation

Low-cost QCM system platforms based on Arduino microcontroller board mentioned above was designed for detect one QCM sensor resonance frequency change or the differential frequency of two same QCM sensors in gas and liquid phase. The AT-cut 6MHz and 10MHz Ti/ Au-coated QCM sensors were purchased from OpenQCM store, its electrode of a 6 mm diameter circle. And two liquid cells made of Teflon were purchased from International Crystal Manufactory (ICM). A frequency counter (BK precision model 1823A) was employed during the experiments. Electrochemical station (Zahner Zennium PP211) was used in electrochemical experiments. Light generator (Newport model 66902) was chosen for generate UV irradiation during the photocatalytic degradation experiments.

4.3 Procedures

For QCM experiments, coating substrates onto the surface of QCM sensor acts an important role in preparation phase. There are several common methods for coating QCM sensor: 1) drop coating 2) spin coating, and 3) electrophoretic deposition. For the evaporation experiments, drop coating as a simple and easy method has been adopted, and for photocatalytic degradation, electrophoretic deposition is better because of its available and efficient.

Before each experiment, QCM sensor should be rinsed by ethanol and DI water for several times. After air drying, QCM sensors are assembled with oscillator circuit unit one, two or three and Arduino microcontroller board or frequency counter. If the liquid cell was used, it also should be rinsed and dried, and then put QCM sensor inside, using four screws on its bottom to fix it.

- 1) Comparison of three different oscillator circuits to measure 10MHz and 6MHz QCM sensors frequencies with or no cell.

- 2) TiO₂ thin film formation

TiO₂ powder was suspended in methanol in three 40ml beakers; three concentrations of TiO₂ were prepared in 50mg/ml, 10mg/ml, and 5mg/ml respectively. When coating TiO₂, which has a positive charge in methanol, the electrode of QCM sensor was placed at the cathode. Samples were prepared at 1V, 5V, 10V, or 15V for 15s or 30s⁴⁰. After drying in air and cleaning the extra TiO₂ which were out of active area. SEM technique was employed to observe their surface features to find the best coating condition.

3) Methyl orange thin film formation and photocatalysis test

Making 90 mg/L methyl orange solution, using 10uL dropper drop coat one drop on the TiO₂ thin film of QCM surface, drying in the dark. Repeat two or three times to form methyl orange thin film. Using the 210W special white light, which has some UV light along with it, to exposure QCM sensor combined with methyl orange and TiO₂ thin film on the electrode surface. Meanwhile, a thermistor was adopted to measure real-time ambient temperature during the experiment.

4) Oscillator circuit unit three applied to electrochemical test

Connecting the 10MHz QCM sensor with cell to oscillator circuit unit three, it was to measure initial frequency of QCM sensor before adding reagent solution. The working electrode of electrochemical station and the electrode surface which was contacted with solution are connected together to the ground of oscillator circuit unit three. 1.0mM and 5.0mM NaI in 50mM NaClO₄ and 1.0mM and 5.0mM NaBr in 50mM NaClO₄ solution had been prepared for halide adsorption and desorption experiments.

5) Test two oscillator circuit units and difference frequency of each of both without cell

Connect and assemble the QCM system platforms following Figure 4.3.1 and Figure 4.3.2, measuring and save the sensing QCM sensor frequency, reference QCM sensor frequency, and difference frequency between them respectively. Compare the result of calculated frequency of sensing and reference QCM sensor and the result of measured difference frequency.

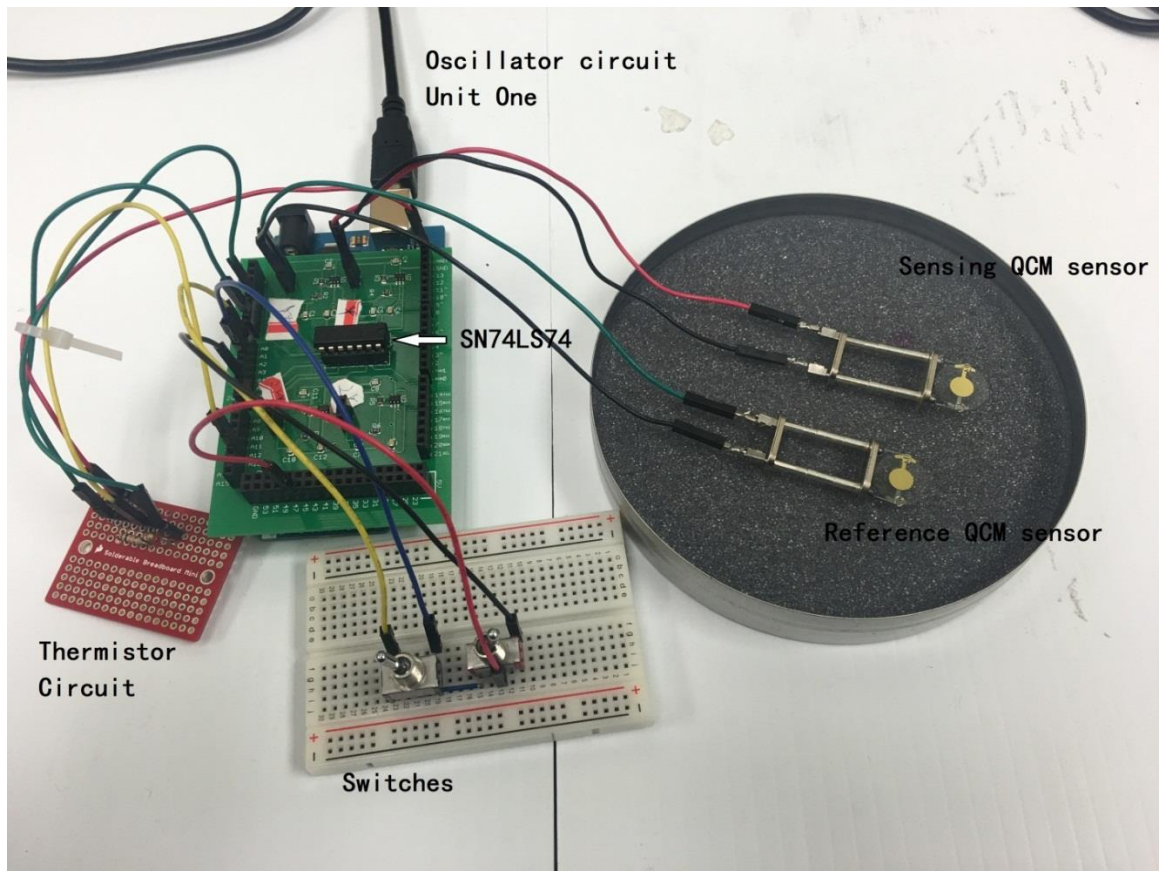


Figure 4.3.1 Oscillator circuit unit one with two QCM sensors

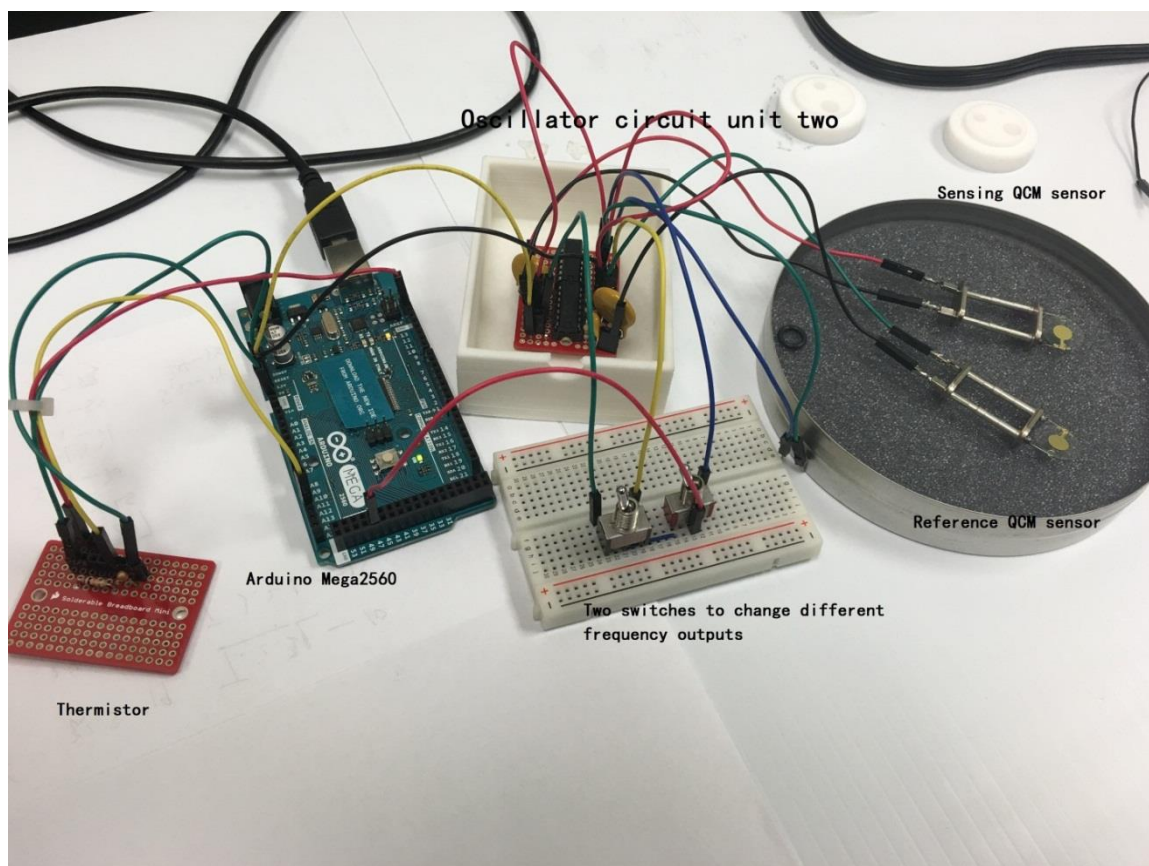


Figure 4.3.2 Oscillator circuit unit two with two QCM sensors

- 6) Ethanol evaporation on one QCM sensor without liquid cell
 - i) Connect Arduino microcontroller board to personal computer and plug one QCM sensor into one of oscillator circuits, then run the QCM system platform for several minutes until the frequency line seems to be stable. And make one drop of 10 μ l anhydrous ethanol onto the surface of QCM sensor, keep it at the room temperature and quiet place with minimum external interference, record one QCM sensor itself resonance frequency. After 5-10mins, repeat the steps several times, capture the image and save the frequency data.

- ii) Connect Arduino microcontroller board to personal computer and plug two QCM sensors into the left or right side of oscillator circuits, as shown in Figure 4.3.1. Then run the QCM system platform for several time until the frequency line seems to be stable. And make one drop of anhydrous ethanol onto one surface of two QCM sensors, the other is as reference sensor, keep them at the room temperature and quiet place without external interference, record the differential resonance frequency of two QCM sensor. After 5-10mins, repeat the steps several times, capture the image and save the frequency data.
- 7) The study on the photocatalytic degradation processing of Rhodamine B (RB) at the Surface of nanocrystalline TiO_2 by QCM sensor.

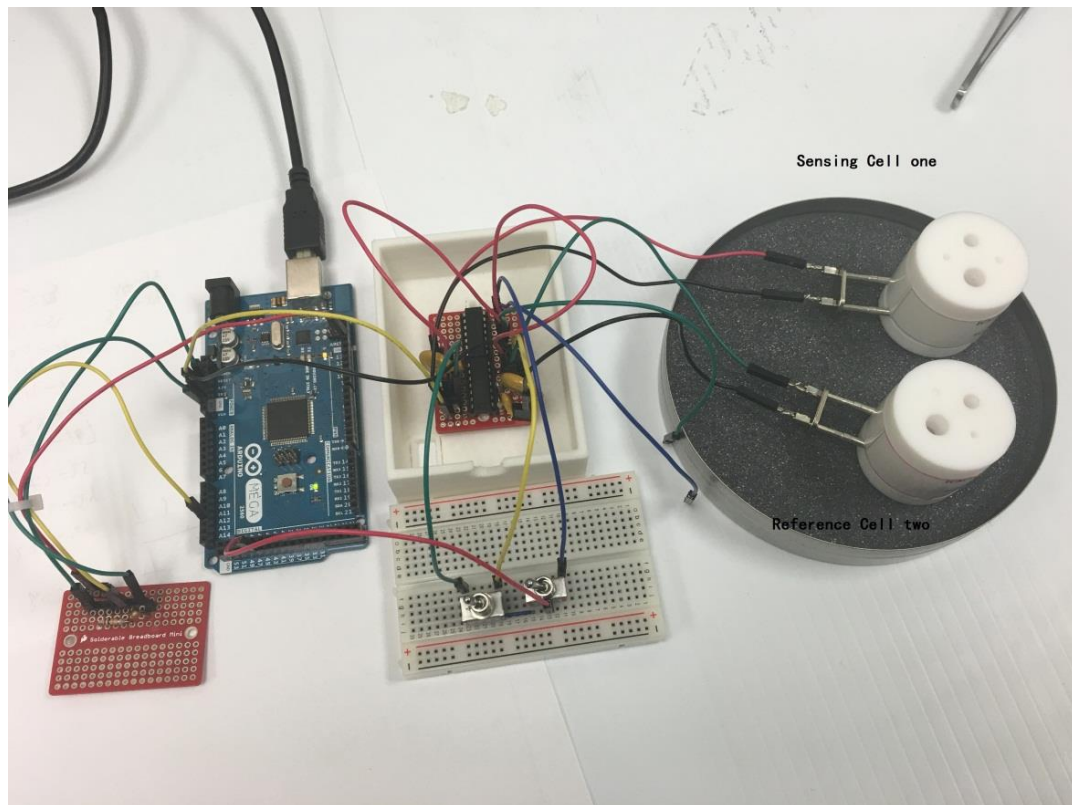


Figure 4.3.3 photocatalytic degradation processing of Rhodamine B (RB) at the Surface of nanocrystalline TiO₂

After cleaning the electrode surface by anhydrous ethanol and DI water, QCM sensor is fixed in the cell. TiO₂ nano-film is made by drop-coating method, and then put the cell into drying box. After 5 minutes, take the cell out of drying box and connect to the QCM system platform, measuring the frequency of QCM sensor with TiO₂ nano-film until the frequency reach a stable range. Thus, 2 ml of Rhodamine B is injected into the cell, and move the cell under the natural light for several hours. Frequency data are acquired continuously and saved. In order to detect that graphene can affect the speed of photocatalysis of Rhodamine B and TiO₂, graphene is added to TiO₂ solution and form TiO₂-GP mixed solution. And following steps are the same as ones above.

Result and discussion

5.1 Comparison of three different oscillator circuits to measure 10MHz and 6MHz QCM sensors frequencies with or no cell.

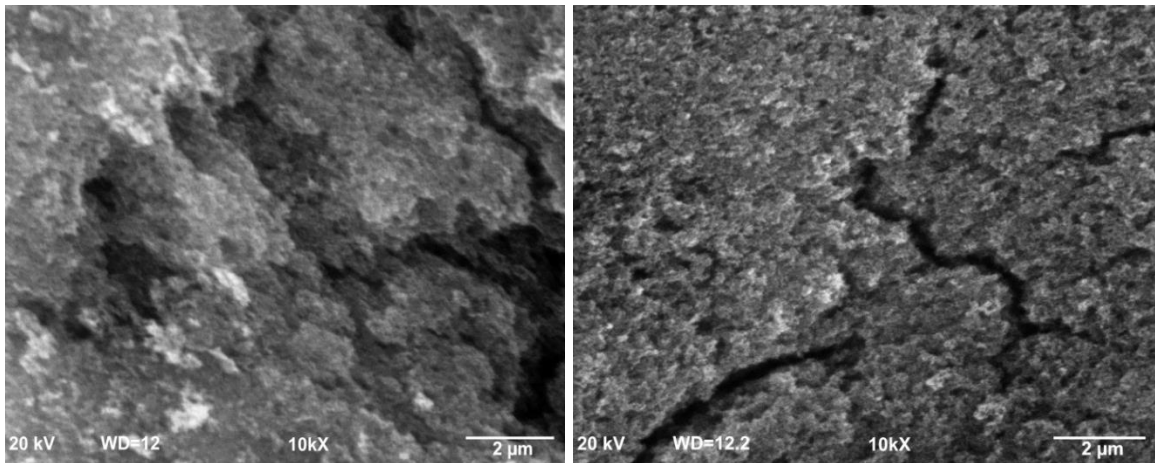
Table 5.1.1 Comparison of three circuits QCM sensors frequency measured by frequency counter

Oscillator circuit	10MHz no cell	6MHz no cell	10MHz with cell	6MHz with cell
Unit one	10.01526MHz	6.015015MHz	10.01487MHz	6.014782MHz
Unit two	10.01854MHz	6.016123MHz	10.01845MHz	unavailable
Unit three	10.01326MHz	6.012326MHz	10.01321MHz	unavailable

From Table 5.1.1, 10MHz QCM sensor's frequency was stable with or without cell, but 6MHz QCM sensor's frequency was stable without cell and only stable will cell in oscillator circuit unit one.

5.2 Morphology of TiO₂ coating

Electrophoretic deposition as an available and efficient method for coating TiO₂ on QCM sensor, suspension solvent and concentration both played a very important role in affecting the coating morphology⁴⁰. Based on different concentration, deposition voltage, and time, TiO₂ could form thin films on electrode surface in different thickness. After measuring the before and after coating TiO₂ frequency of QCM sensor, and compared with SEM features, the better condition is 5mg/ml TiO₂ in methanol with 5V voltage under 15s which can form a frequency-measurable TiO₂ thin film.



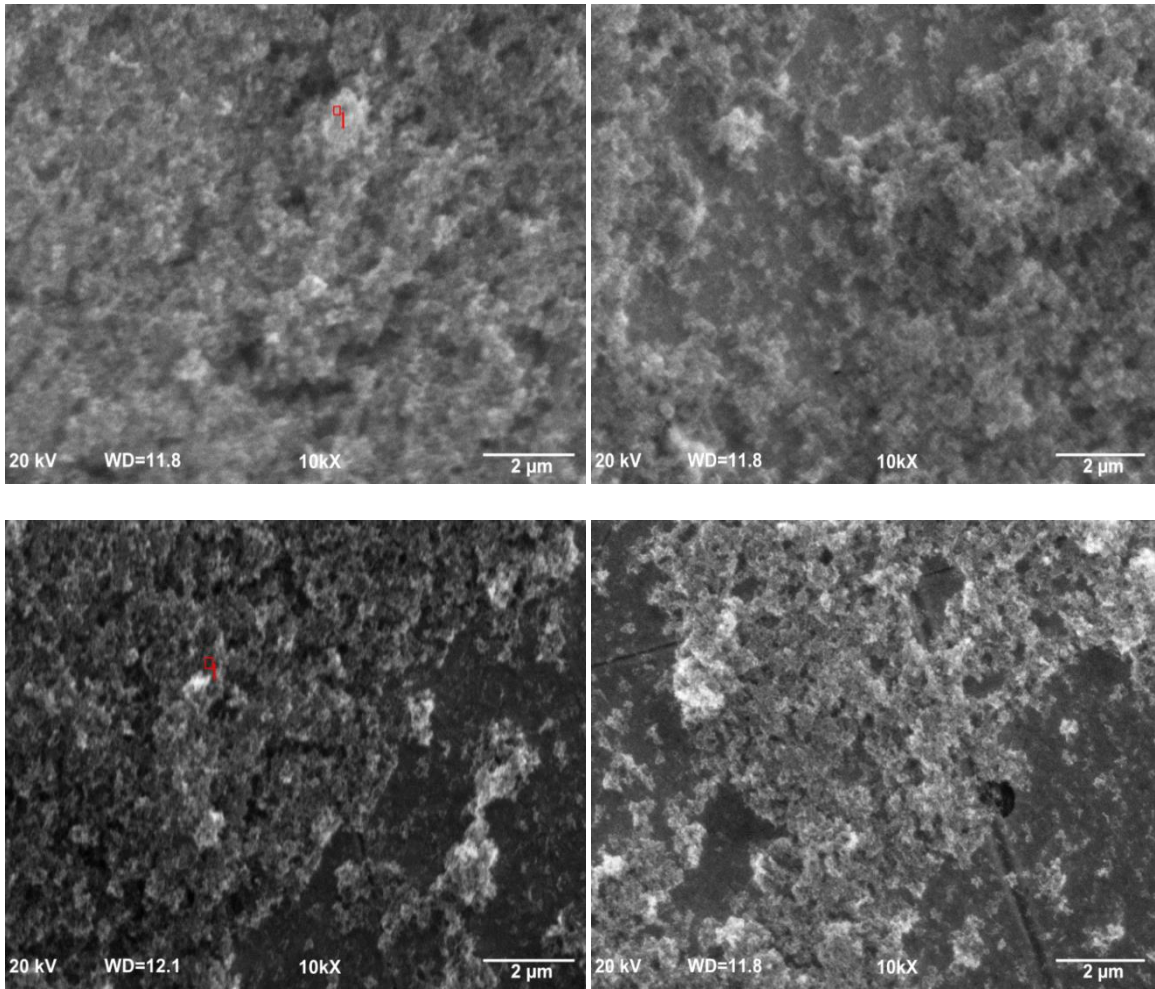


Figure 5.2.1 SEM scanned features of 10mg/ml, 15V, 30s; 5mg/ml, 10V, 30s; 5mg/ml, 5V, 30s; 5mg/ml, 5V, 15s; 50mg/ml, 1V, 15s; and 5mg/ml, 1V, 30s TiO₂ electrophoretic deposition

Electrophoretic deposition was under 10mg/ml, 15V, 30s; 5mg/ml, 10V, 30s; and 5mg/ml, 5V, 30s, the TiO₂ films were so a little thicker that their frequencies could not be measured in reasonable range. On the contrary, under 50mg/ml, 1V, 15s and 5mg/ml, 1V, 30s, the TiO₂ film were too thinner and distributed too unevenly. After comparison, 5mg/ml, 5V, 15s is a desired condition for electrophoretic deposition. For example, a

6MHz and a 10MHz QCM sensor were coated TiO₂ under 5mg/ml, 5V, 15s condition (as shown Table 5.2.1).

Table 5.2.1 Comparison of 6MHz and 10MHz QCM sensor coating TiO₂ film

f_0	Δf	Δm
6.011813MHz	7205Hz	24.497ug/cm ²
10.01543MHz	19186Hz	23.791ug/cm ²

5.3 Methyl orange light degradation

To make methyl orange thin film on TiO₂-coated QCM sensor, two drops were on 6MHz QCM and three drops were on 10MHz QCM. The mass of methyl orange is shown in Table 5.3.1. Under 210W white light along with UV light, both frequencies were increasing with time (as shown in Figure 5.3.1 and Figure5.3.2).

Table 5.3.1 Comparison of 6MHz and 10MHz TiO₂-coated QCM sensor coating methyl orange film

f_1	Δf_1	Δm_1
6.004608MHz	168Hz	571.2ng/cm ² (two drops)
9.996244MHz	635Hz	787.4ng/cm ² (three drops)

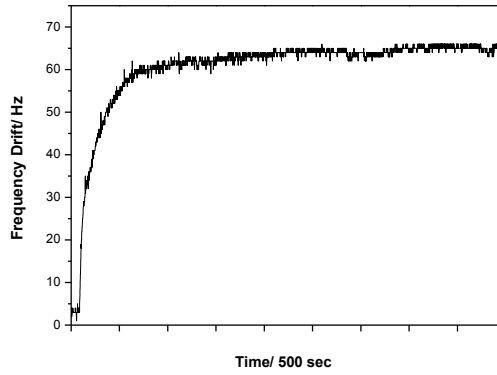


Figure 5.3.1 Photocatalytic degradation of 6MHz methyl orange-TiO₂-coated QCM sensor

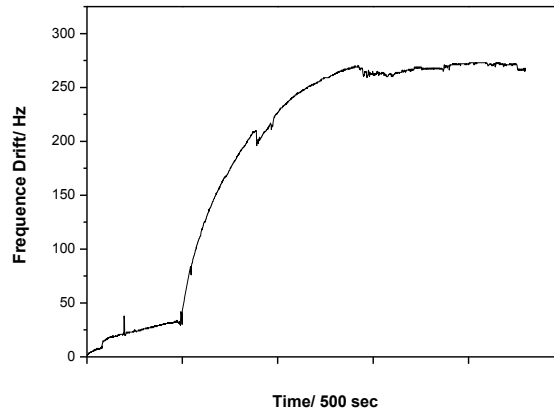


Figure 5.3.2 Light degradation of 10MHz methyl orange-TiO₂-coated QCM sensor

Table 5.3.2 Comparison of 6MHz and 10MHz photocatalytic degradation

f_2	Δf_2	Δm_2
6.004440MHz	67Hz	227.8ng/cm ² (two drops)
9.995606MHz	275Hz	341ng/cm ² (three drops)

For 90mg/l methyl orange solution, 10ul dropper could make around 3 drops, after calculation, the masses of methyl orange before photocatalytic degradation were close to the value measured by QCM system. But after photocatalytic degradation, the masses of methyl orange were smaller than the ones calculated before. One assumption was that after photocatalytic degradation, some degradation productions of methyl orange were left on the TiO_2 – coated QCM sensor surface due to frequencies not increasing to the initial values. For instance, molecule of methyl orange had $-\text{SO}_3\text{H}$, under the photocatalyst, it turned to SO_4^{2-} which was left on the QCM sensor, and other elements (N, C, H, etc.) were gone in gas state.

5.4 Oscillator circuit unit three applied to electrochemical test

Using oscillator circuit unit three, measure 10MHz QCM sensor initial frequency with cell, which has been mention in 5.1. Because of complexity of liquid phase in QCM application, the measured frequencies were too much unstable and swift changed up and down in several thousand Hz after injecting the reagent solutions. Even though unexpected drift exist, the trend of frequency was in right direction. However, it extremely influenced the precision of measurement. There was a big challenge to figure out QCM sensor stably vibrating in liquid phase. Fortunately, when the oscillator circuit unit one connected to electrochemical station, they did not affect their functions each other. Therefore, more efforts need to do to improve oscillator circuit function to overcome the problems in QCM liquid applications.

5.5 Test two oscillator circuit units and difference frequency of each of both without cell

Testing oscillator circuit unit one and two with Arduino microcontroller board, the stabilities of two QCM system platforms are a little different in gas phase. From Figure 5.5.1 to Figure 5.5.4, in oscillator circuit unit one, the range of each frequency signal is around 9 Hz, which is a little more than the one in oscillator circuit unit two. And the values of the same QCM sensor are different by measured with unit one and two. Because they use different electronic components and are influenced by wire connections, limitation of components, and so on. Compared the value of difference frequency measured and calculated, the ranges are around 3 – 6.5Hz, the result is acceptable.

See Figure 5.5.3, two separated QCM sensors frequency were measured, sensor 1 f_1 is around 6.025046 MHz, sensor 2 f_2 is around 6.015250 MHz, so the differential frequency f of f_1 and f_2 is around 9796 Hz. From comparison of measurement of f with the difference of $f_1 - f_2$, it is very clearly to be seen in Figure 5.5.4, the fluctuation range is 3-4 Hz, which can illustrate that the differential frequency oscillator circuit works in the desired condition.

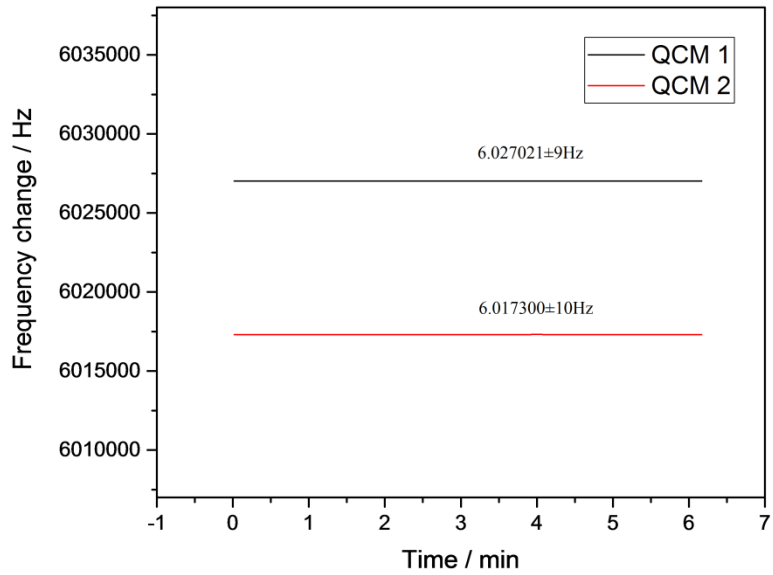


Figure 5.5.1 Frequencies of two QCM sensors in unit one

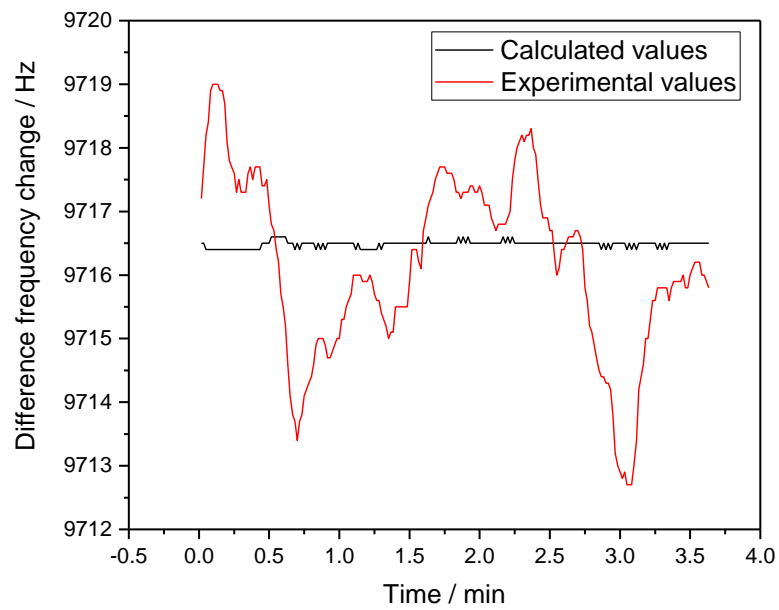


Figure 5.5.2 Calculated values VS experimental values in unit one

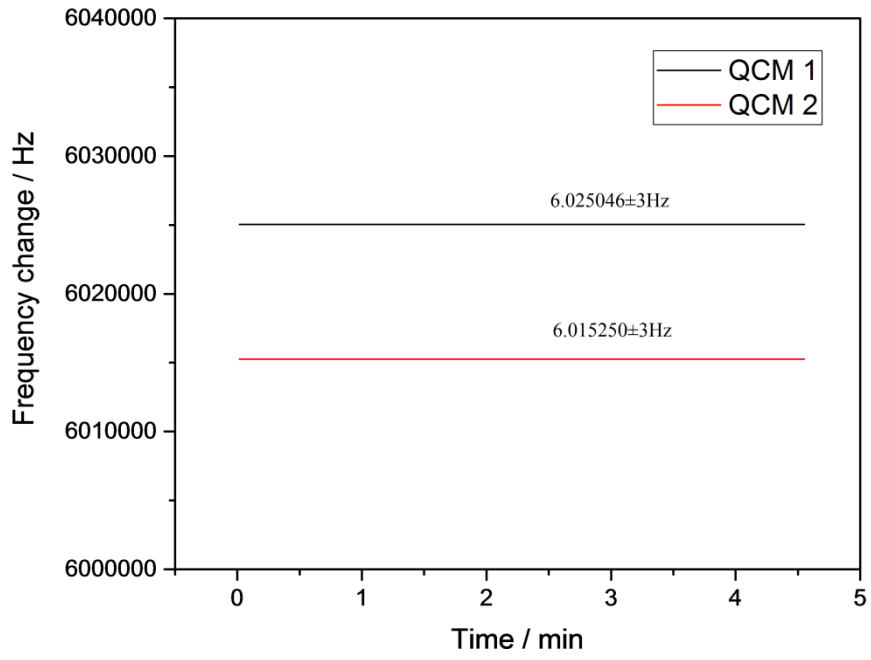


Figure 5.5.3 Frequencies of two QCM sensors in unit two

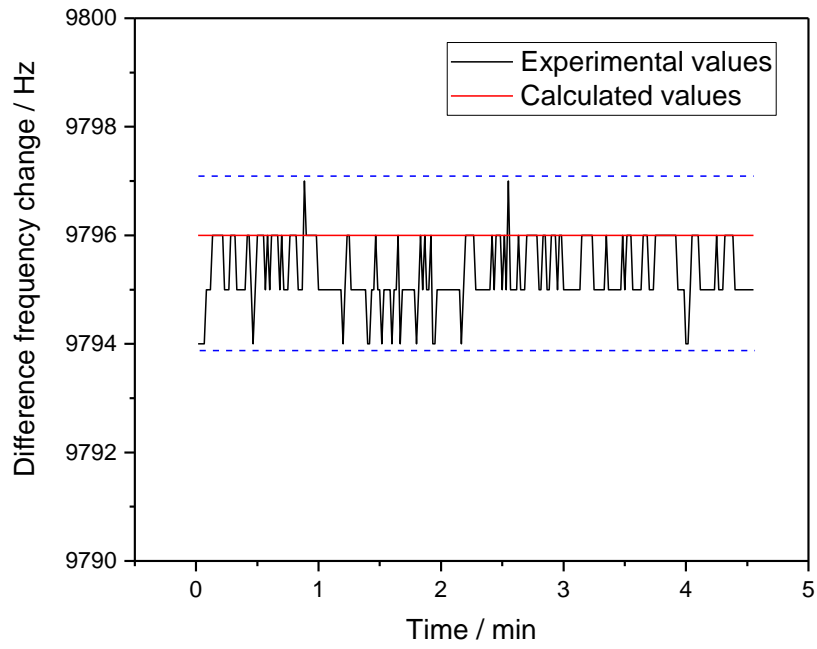


Figure 5.5.4 Calculated values VS experimental values in unit two

5.6 Ethanol evaporation on one QCM sensor without liquid cell

See Figure 5.6.1, in the ethanol evaporation experiment, the QCM sensor was firstly measured to get its frequency value which was around 6.0155MHz, after one drop ethanol on the surface, the frequency decreased with time by the lowest point. With evaporation of ethanol, totally around 2-3mins, the frequency of QCM sensor turned back to the initial value. By five times tests, the waves of frequency change were almost same ($\Delta f \approx 1212\sim 1307$ Hz), so it could be identified that the amount of each drop of ethanol is the same. Based on Sauerbrey equation, the mass of one drop of ethanol could be calculated. Substitute the parameters into equation 13, the value of the mass of one drop ethanol $\Delta m \approx 4.138\sim 4.443\mu\text{g}$. Due to one drop of ethanol laid on the surface of QCM sensor; it could not form rigid film. Based on the Sauerbrey's theory, even though there showed the frequency decreasing and turning back to initial frequency, it did not mean that the mass calculated by the frequency swift was equal to the actual mass of one drop of ethanol. The result could prove it.

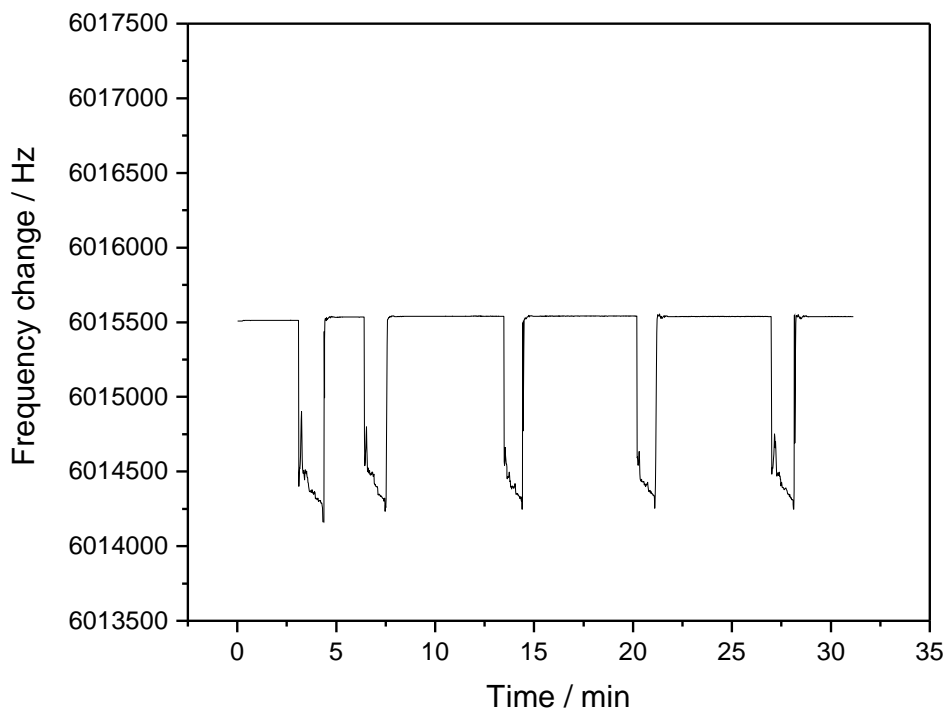


Figure 5.6.1 Ethanol evaporation on one QCM sensor without liquid cell

5.7 The study on the photocatalytic degradation processing of Rhodamine B (RB) at the Surface of nanocrystalline TiO₂ by QCM sensor

Compared Figure 5.7.1 and 5.6.2, they clearly illustrate that after injecting 2 ml of Rhodamine B solution, the both frequencies were increasing by over 3.35 MHz, it is because the reaction system of the QCM sensor was changed for gas to liquid, the main effect factors to QCM sensor are viscosity and density of solution. In addition, according to equation 14, Δf is proportional to $(\rho_1 \eta_1)^{1/2}$, the viscosity and density of solution are much more than the ones of air, so the frequency is increasing to the high point. With the reaction of the photocatalytic degradation processing of Rhodamine B

(RB) at the Surface of nanocrystalline TiO_2 , the viscosity and density of solution decreased so that the frequency is also decreasing. In Figure 5.7.2, the frequency of QCM sensor seems stable after around 500 minutes, however, the frequency of QCM sensor in Figure 5.6.3 reaches the stable status after around 300 minutes. This difference illustrates graphene which added into TiO_2 solution can improve the speed of photocatalytic degradation processing of Rhodamine B with TiO_2 as the photocatalyst.

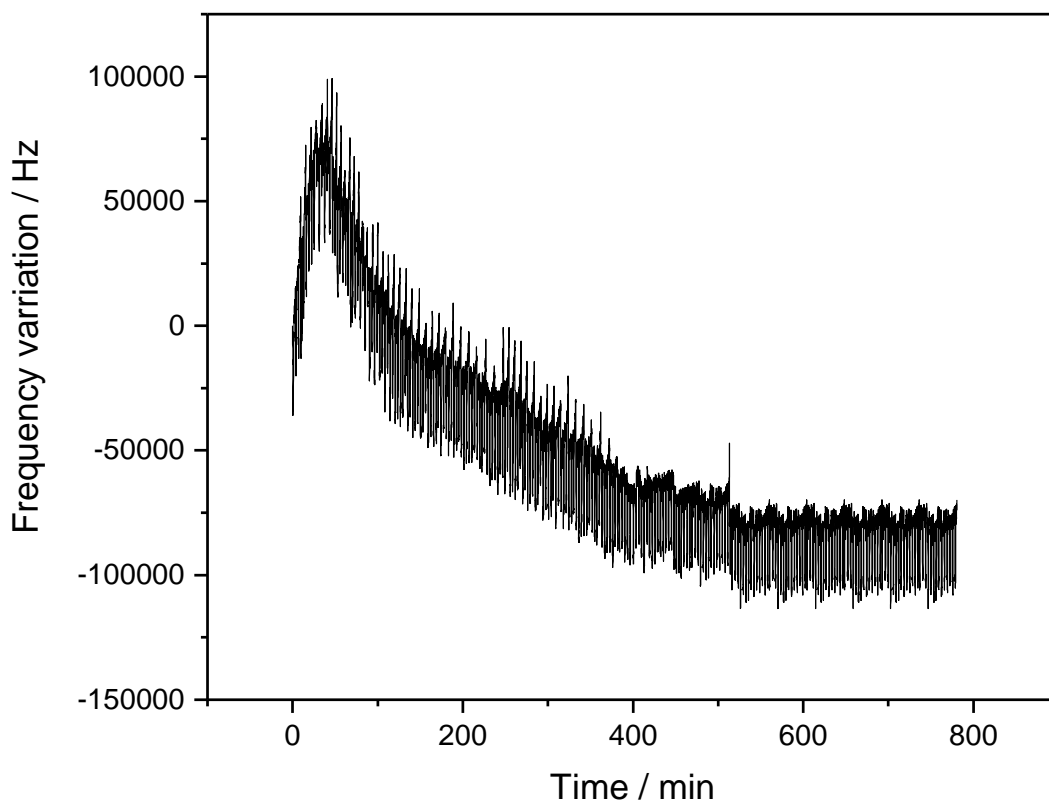


Figure 5.7.1 Photocatalytic degradation processing of Rhodamine B (RB) at the Surface of nanocrystalline TiO_2

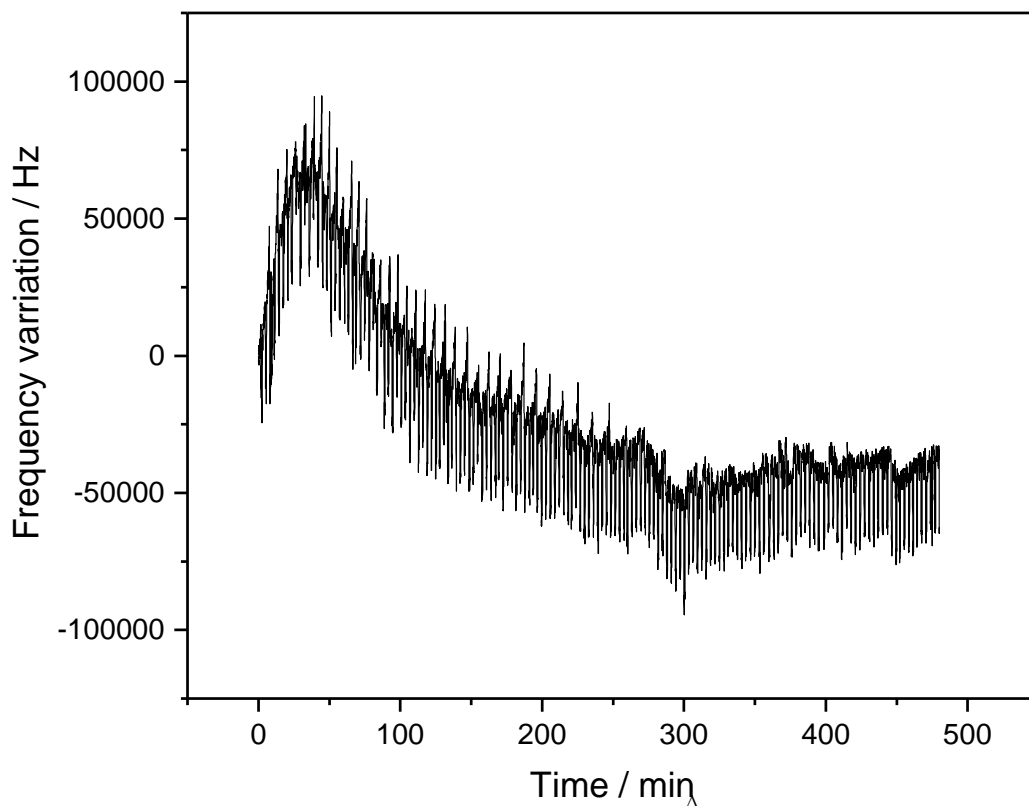


Figure 5.7.2 Photocatalytic degradation processing of Rhodamine B (RB) at the Surface of nanocrystalline TiO₂-GP

Other equipment designed with Arduino microcontroller board

Arduino microcontroller board as a multi-functional and cheap integrated circuit board has been applied into variable scientific fields. Due to its functional diversification, it can control stepper motors, acquire signals from sensors, and combine with some interface software to achieve real-time monitor. It is so convenient that users can design

their own devices by programming for Arduino microcontroller board. The following systems are designed with Arduino boards.

- Multi-channel valves array system controlled by Arduino with Labview interface
In this system, users can select different routes for what they want by controlling valves open or close. No matter what gas or liquid, they should be found their ways to go through the tubes (as shown in Figure 6.1).
- Adjustable micro-doses injection system for monolayer film formation system
By controlling stepper motor's stepper speed, to push down or pull up syringe to output tiny amount of reagent solution as tiny as 0.52nl/s (as shown in Figure 6.4).
- Thermogravimetric analysis (TGA) system with quartz crystal microbalance
TGA with QCM system can improve the precision of measurement because of QCM can be sensitive to nanogram level. Arduino boards were used to record the real-time temperatures of thermocouples from oven and QCM ambient temperature, and measure real-time frequency swift of QCM sensor. A fan will work for heat dissipation after experiment is done (as shown in Figure 6.5).

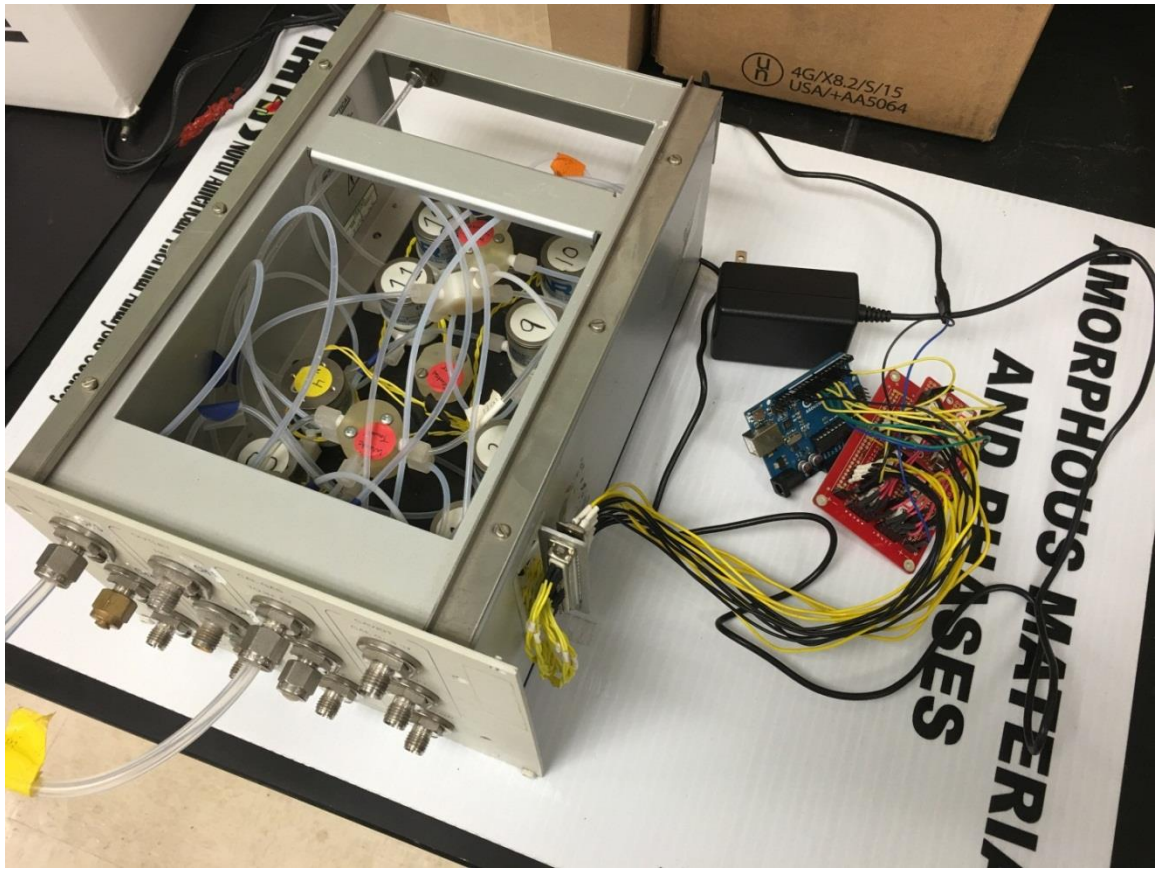


Figure 6.1 Multi-channel valves array system

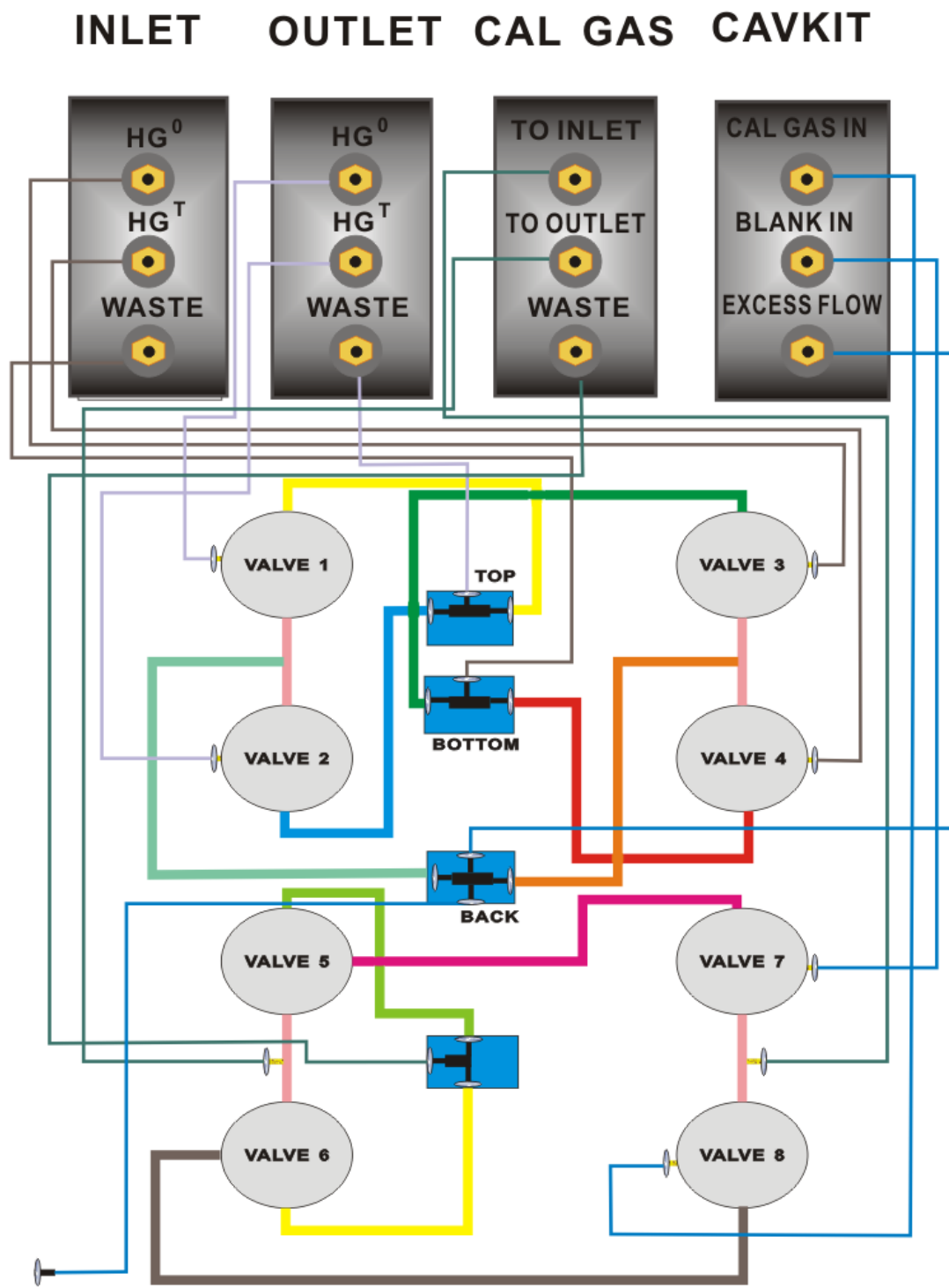


Figure 6.2 Logic diagram for multi-channel valves array system

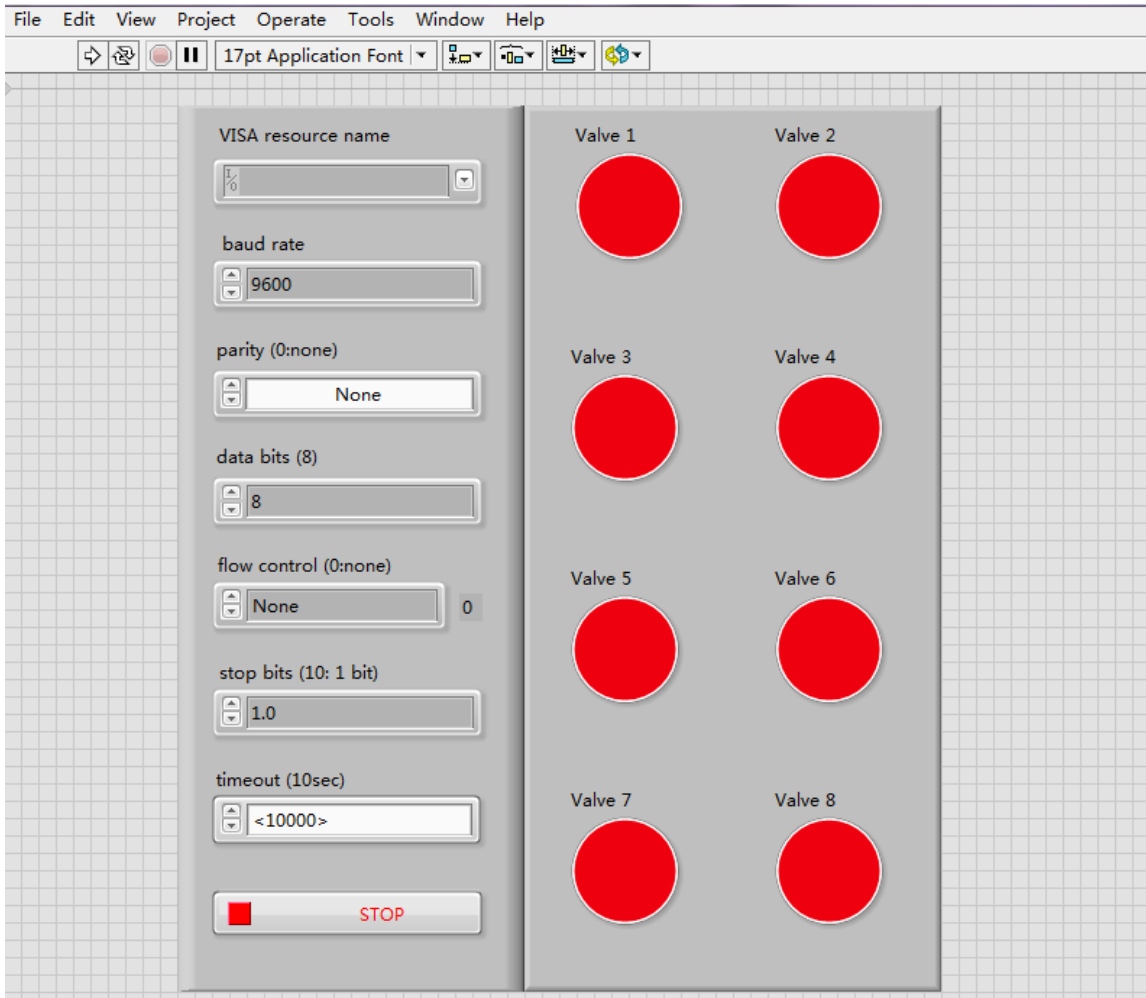


Figure 6.3 Labview interface for Multi-channel valves array system

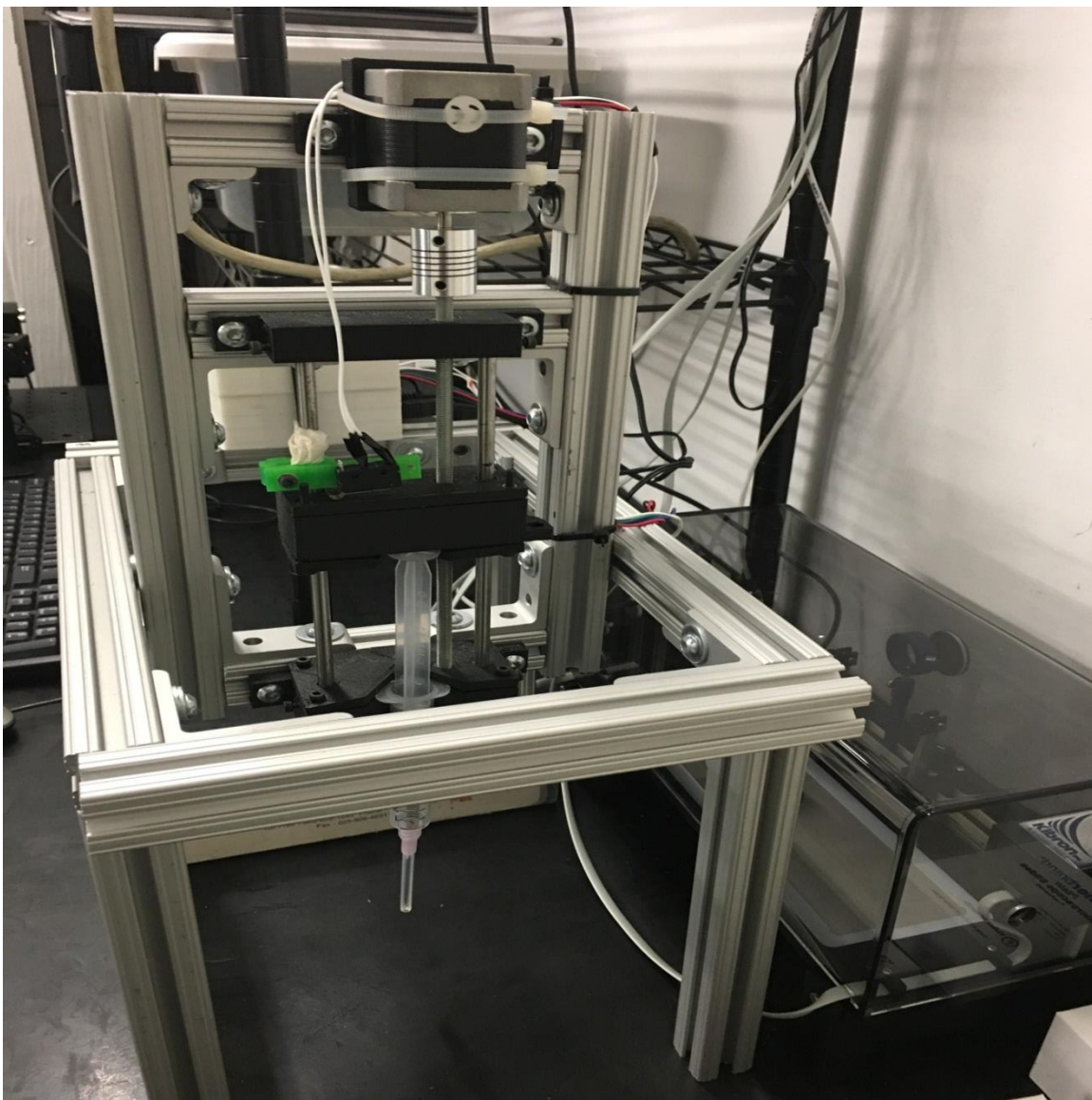


Figure 6.4 Adjustable micro-doses injection system for monolayer film formation system

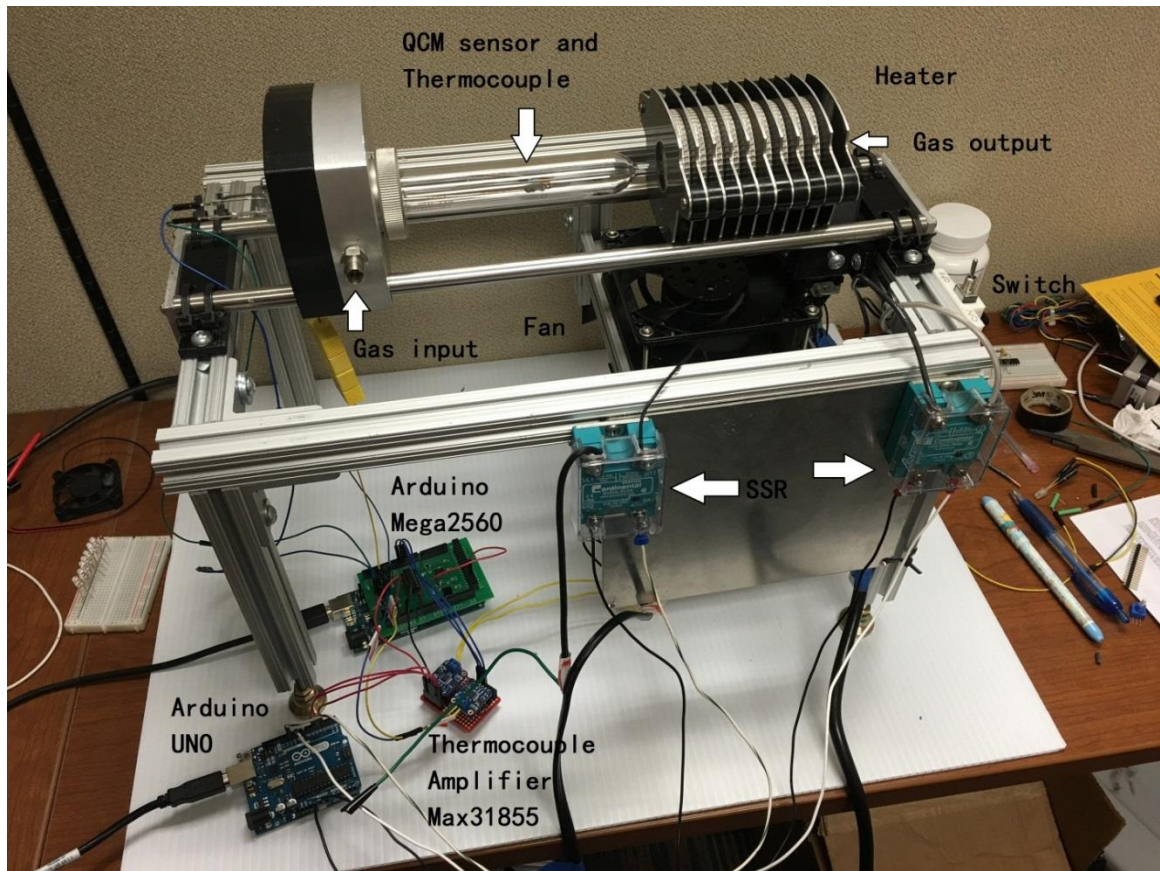


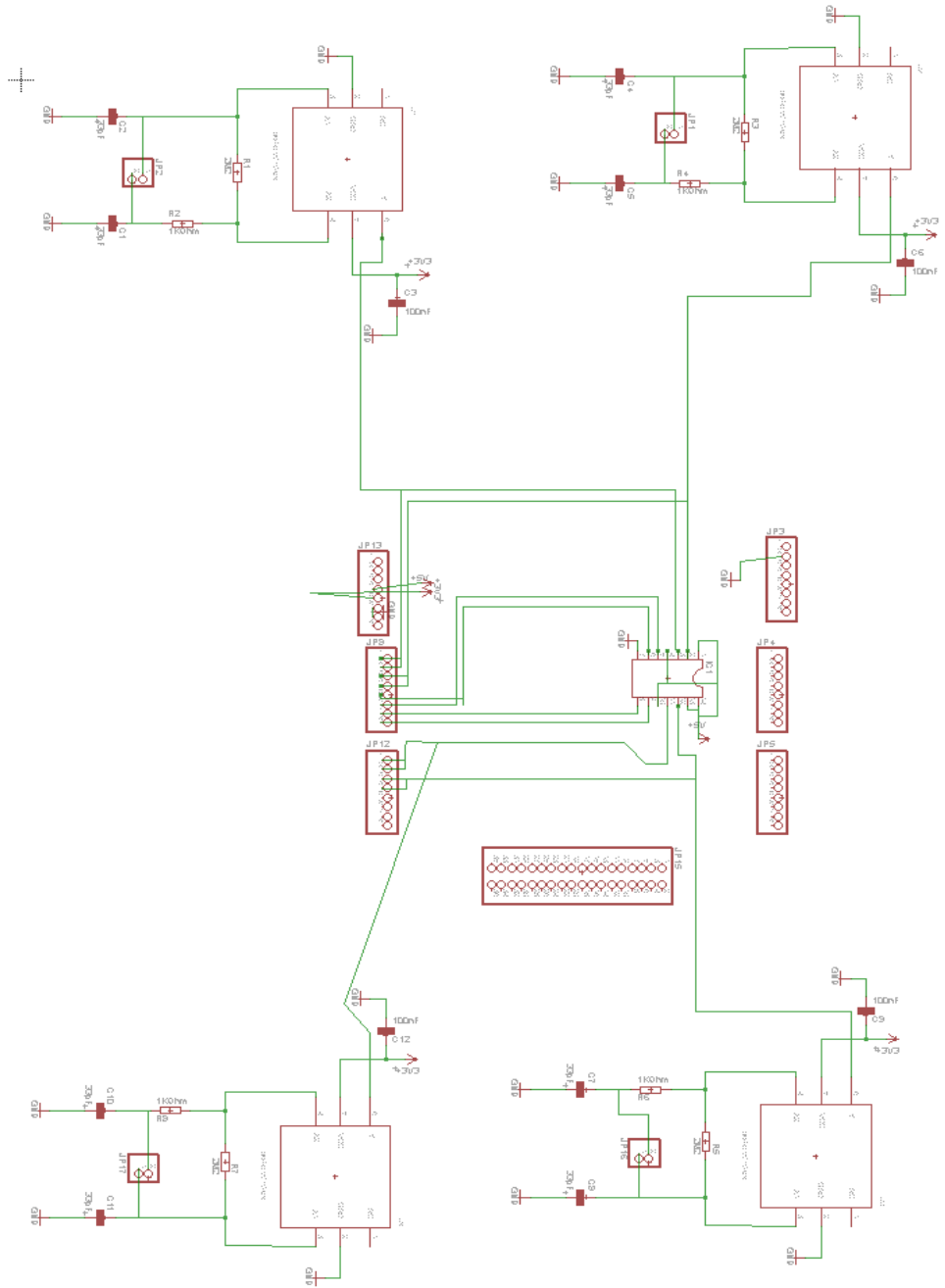
Figure 6.5 Thermogravimetric analysis system with quartz crystal microbalance

Conclusion

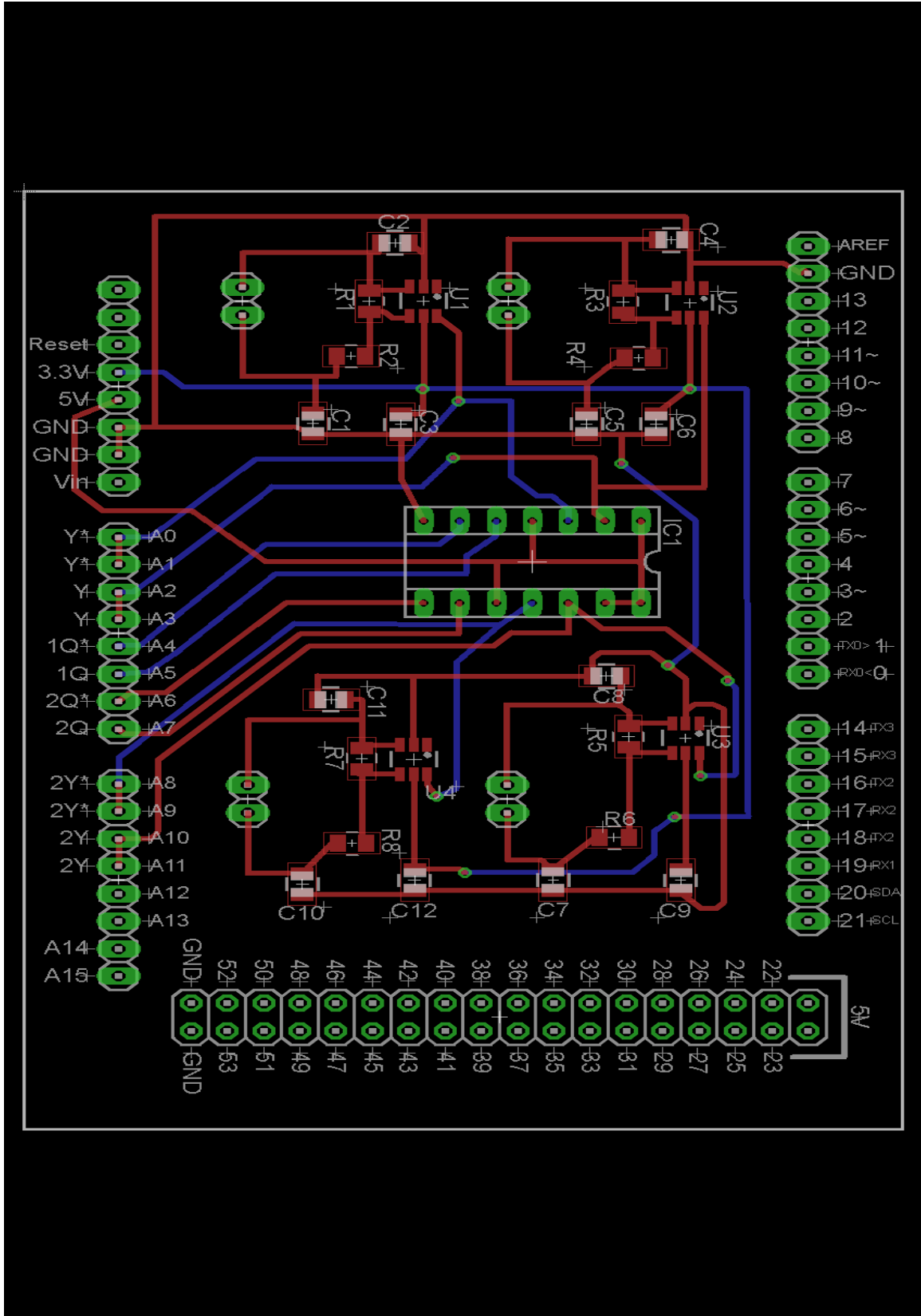
Quartz crystal microbalance sensor has excellent advantages of high sensitivity coefficient, measuring tiny mass change in nanogram level, and relative physical and mechanical properties. QCM sensor can detect micro-world change because it works based on the sensitive film on the surface as sensitive component, the AT-cut quartz crystal as transducer component, according to the change relationship between mass and frequency, the tiny mass signal can be transduced to frequency signal. Depended on QCM sensor properties, this article mainly states that low-cost QCM system platforms

are designed with Arduino microcontroller board, three simple-construction, low-cost difference frequency oscillator circuit units were designed and used some simple and representative experiments to detect how the platforms perform. For the coating methods, electrophoretic deposition was much better than drop coating. Methyl orange light degradation with TiO_2 worked successfully matching Sauerbrey's theory and equation, which had proved that the QCM systems could come to use in gas phase. However, due to extreme frequency drift in liquid phase, QCM system for liquid application should be improved and enhanced. It needs to be more explored. Two setup platforms which were working for gas phase and liquid phase exist its own weaknesses, which need to continuously improved and enhanced, like stability and sensitivity of oscillator circuits, reducing the effect factors of temperature, viscosity and density of liquid. The oscillator circuit should be added more functional components, like filter, inductor, amplifier, and so on, to work in gas and liquid phase better.

APPENDIX A: OSCILLATOR CIRCUIT SCHEMATIC DIAGRAM



APPENDIX B: OSCILLATOR CIRCUIT PCB BOARD SCHEMATIC DIAGRAM



APPENDIX

APPENDIX A: OSCILLATOR CIRCUIT SCHEMATIC DIAGRAM.....65

APPENDIX B: OSCILLATOR CIRCUIT PCB BOARD SCHEMATIC DIAGRAM...66

LITERATURE CITED

1. Curie, J.; Curie, P., Développement, par pression, de l'électricité polaire dans les cristaux hémihédres à faces inclinées. *Comptes Rendus* **1880**, *91*, 294-295.
2. Gautschi, D.-I. E. G., *Piezoelectric sensors*. Springer: 2002.
3. Sauerbrey, G., Verwendung von Schwingquarzen zur Wägung dünner Schichten und zur Mikrowägung. *Zeitschrift für physik* **1959**, *155* (2), 206-222.
4. King Jr, W. H., Piezoelectric Sorption Detector. *Analytical Chemistry* **1964**, *36* (9), 1735-1739.
5. (a) Alder, J. F.; McCallum, J. J., Piezoelectric crystals for mass and chemical measurements. A review. *Analyst* **1983**, *108* (1291), 1169-1189; (b) McCallum, J. J., Piezoelectric devices for mass and chemical measurements: an update. A review. *Analyst* **1989**, *114* (10), 1173-1189.
6. Guilbault, G. G., Determination of formaldehyde with an enzyme-coated piezoelectric crystal detector. *Analytical Chemistry* **1983**, *55* (11), 1682-1684.
7. Ngeh-Ngwainbi, J.; Foley, P.; Kuan, S. S.; Guilbault, G., Parathion antibodies on piezoelectric crystals. *Journal of the American Chemical Society* **1986**, *108* (18), 5444-5447.
8. Shons, A.; Dorman, F.; Najarian, J., An immunospecific microbalance. *Journal of biomedical materials research* **1972**, *6* (6), 565-570.
9. Plomer, M.; Guilbault, G. G.; Hock, B., Development of a piezoelectric immunosensor for the detection of enterobacteria. *Enzyme and Microbial Technology* **1992**, *14* (3), 230-235.

10. He, F.; zhu, W.; Geng, Q.; Nie, L.; Yao, S., Rapid detection of Escherichia coliform using a series electrode piezoelectric crystal sensor. *Analytical letters* **1994**, *27* (4), 655-669.
11. Carter, R.; Mekalanos, J.; Jacobs, M.; Lubrano, G.; Guilbault, G., Quartz crystal microbalance detection of Vibrio cholerae O139 serotype. *Journal of immunological methods* **1995**, *187* (1), 121-125.
12. König, B.; Grätzel, M., A piezoelectric immunosensor for hepatitis viruses. *Analytica chimica acta* **1995**, *309* (1), 19-25.
13. Rickert, J.; Weiss, T.; Kraas, W.; Jung, G.; Göpel, W., A new affinity biosensor: self-assembled thiols as selective monolayer coatings of quartz crystal microbalances. *Biosensors and Bioelectronics* **1996**, *11* (6), 591-598.
14. Sakai, G.; Saiki, T.; Uda, T.; Miura, N.; Yamazoe, N., Selective and repeatable detection of human serum albumin by using piezoelectric immunosensor. *Sensors and Actuators B: Chemical* **1995**, *24* (1), 134-137.
15. Muramatsu, H.; Kajiwara, K.; Tamiya, E.; Karube, I., Piezoelectric immuno sensor for the detection of Candida albicans microbes. *Analytica chimica acta* **1986**, *188*, 257-261.
16. Konash, P. L.; Bastiaans, G. J., Piezoelectric crystals as detectors in liquid chromatography. *Analytical Chemistry* **1980**, *52* (12), 1929-1931.
17. Nomura, T.; Okuhara, M., Frequency shifts of piezoelectric quartz crystals immersed in organic liquids. *Analytica Chimica Acta* **1982**, *142*, 281-284.
18. Kanazawa, K. K.; Gordon, J. G., The oscillation frequency of a quartz resonator in contact with liquid. *Analytica Chimica Acta* **1985**, *175*, 99-105.

19. Bruckenstein, S.; Shay, M., Experimental aspects of use of the quartz crystal microbalance in solution. *Electrochimica Acta* **1985**, *30* (10), 1295-1300.
20. Schmitt, N.; Tessier, L.; Watier, H.; Patat, F., A new method based on acoustic impedance measurements for quartz immunosensors. *Sensors and Actuators B: Chemical* **1997**, *43* (1), 217-223.
21. Bizet, K.; Gabrielli, C.; Perrot, H.; Therasse, J., Validation of antibody-based recognition by piezoelectric transducers through electroacoustic admittance analysis. *Biosensors and Bioelectronics* **1998**, *13* (3), 259-269.
22. Okahata, Y.; Kawase, M.; Niikura, K.; Ohtake, F.; Furusawa, H.; Ebara, Y., Kinetic measurements of DNA hybridization on an oligonucleotide-immobilized 27-MHz quartz crystal microbalance. *Analytical Chemistry* **1998**, *70* (7), 1288-1296.
23. Schmitt, R. F.; Allen, J. W.; Vetelino, J. F.; Parks, J.; Zhang, C., Bulk acoustic wave modes in quartz for sensing measurand-induced mechanical and electrical property changes. *Sensors and Actuators B: Chemical* **2001**, *76* (1), 95-102.
24. Kanazawa, K. K., Steady state and transient QCM solutions at the metal| solution interface. *Journal of Electroanalytical Chemistry* **2002**, *524*, 103-109.
25. Welsch, W.; Klein, C.; Von Schickfus, M.; Hunklinger, S., Development of a surface acoustic wave immunosensor. *Analytical chemistry* **1996**, *68* (13), 2000-2004.
26. Wessa, T.; Rapp, M.; Ache, H., New immobilization method for SAW-biosensors: covalent attachment of antibodies via CNBr. *Biosensors and Bioelectronics* **1999**, *14* (1), 93-98.
27. Dahint, R.; Grunze, M.; Josse, F.; Renken, J., Acoustic plate mode sensor for immunochemical reactions. *Analytical Chemistry* **1994**, *66* (18), 2888-2892.

28. Dahint, R.; Seigel, R. R.; Harder, P.; Grunze, M.; Josse, F., Detection of non-specific protein adsorption at artificial surfaces by the use of acoustic plate mode sensors. *Sensors and Actuators B: Chemical* **1996**, *36* (1), 497-505.
29. Kovacs, G.; Vellekoop, M.; Haueis, R.; Lubking, G.; Venema, A., A Love wave sensor for (bio) chemical sensing in liquids. *Sensors and Actuators A: Physical* **1994**, *43* (1), 38-43.
30. Harding, G.; Du, J.; Dencher, P.; Barnett, D.; Howe, E., Love wave acoustic immunosensor operating in liquid. *Sensors and Actuators A: Physical* **1997**, *61* (1), 279-286.
31. Bechmann, R., Frequency-temperature-angle characteristics of AT-type resonators made of natural and synthetic quartz. *Proceedings of the IRE* **1956**, *44* (11), 1600-1607.
32. Marx, K. A., Quartz crystal microbalance: a useful tool for studying thin polymer films and complex biomolecular systems at the solution-surface interface. *Biomacromolecules* **2003**, *4* (5), 1099-120.
33. Eichelbaum, F.; Borngräber, R.; Schröder, J.; Lucklum, R.; Hauptmann, P., Interface circuits for quartz-crystal-microbalance sensors. *Review of Scientific Instruments* **1999**, *70* (5), 2537.
34. Srivastava, A.; Sakthivel, P., Quartz-crystal microbalance study for characterizing atomic oxygen in plasma ash tools. *Journal of Vacuum Science & Technology A* **2001**, *19* (1), 97-100.

35. Guilbault, G.; Lu, S.; Czanderna, A., Application of piezoelectric quartz crystal microbalances. *Methods and Phenomena, Their Applications in Science and Technology* **1984**, 7, 251.
36. Buttry, D. A.; Ward, M. D., Measurement of interfacial processes at electrode surfaces with the electrochemical quartz crystal microbalance. *Chemical Reviews* **1992**, 92 (6), 1355-1379.
37. Lin, Z.; Ward, M. D., Determination of contact angles and surface tensions with the quartz crystal microbalance. *Analytical Chemistry* **1996**, 68 (8), 1285-1291.
38. Mabbott, G. A., Teaching Electronics and Laboratory Automation Using Microcontroller Boards. *Journal of Chemical Education* **2014**, 91 (9), 1458-1463.
39. Buttry, D. A. *Applications of the quartz crystal microbalance to electrochemistry*; DTIC Document: 1989.
40. Torrey, J. D.; Kirschling, T. L.; Greenlee, L. F., Processing and characterization of nanoparticle coatings for quartz crystal microbalance measurements. *Journal of research of the National Institute of Standards and Technology* **2015**, 120, 1.